

UNIVERSITY OF LJUBLJANA

Faculty of Mechanical Engineering

**Razvoj rotorja sesalne enote iz polimernega
materiala**

**Engineering design of impeller for vacuum cleaner
motor from polymer material**

A Master's thesis of the second-cycle master's study programme in
MECHANICAL ENGINEERING

Luis Linares Leyva

Ljubljana, June 2018

UNIVERSITY OF LJUBLJANA

Faculty of Mechanical Engineering

**Razvoj rotorja sesalne enote iz polimernega
materiala**

**Engineering design of impeller for vacuum cleaner
motor from polymer material**

A Master's thesis of the second-cycle master's study programme in
MECHANICAL ENGINEERING

Luis Linares Leyva

Advisor: assoc. prof. PhD. Jože Tavčar
Co-advisor: assoc. prof. PhD. Damjan Klobčar

Ljubljana, June 2018

Acknowledgements

First, I would like to thank all the effort and support that I have been able to obtain from my advisor, professor Jože Tavčar. We have maintained a constant flow of information during all the weeks since I started with the project, and whose help and advice have allowed me to modify this document to its final form. I could not leave aside my co-advisor, professor Damjan Klobčar, whose help has allowed me to have a greater knowledge in the field of welding materials, and with which we have had meetings every time that I needed it.

Secondly, I would like to thank the LECAD laboratory and all the people in the department, since they have supported me every time I have needed it, they have treated me as one more, and from the first day, they gave me a computer with all the software and necessary tools to write this work. I would also like to thank the company DOMEL HOLDING d.d., and more specifically, its development engineer Igor Markič, who has provided me with all the information I needed to write this project, and with whom I have maintained contact via email.

Last but not least, I would like to thank my family and my friends for all the support they have given me day after day since I have been in this new city for myself and, even though there have been bad times, I have been able to move forward with this to become in a better student and a better person.

Declaration

I, the undersigned Luis Linares Leyva student from Erasmus Exchange on the Faculty of Mechanical Engineering at the University of Ljubljana, with registration number 70080529, author of the written final work of studies, entitled: Engineering design of impeller for vacuum cleaner motor from polymer material,

DECLARE that

1. The written final work of studies is a result of my independent work;
2. The printed form of the written final work of studies is identical to the electronic form of the written final work of studies;
3. I acquired all the necessary permissions for the use of data and copyrighted works in the written final work of studies and clearly marked them in the written final work of studies;
4. During the preparation of the written final work of studies I acted in accordance with ethical principles and obtained, where necessary, agreement of the ethics commission;
5. I give my consent to the use of the electronic form of the written final work of studies for the detection of content similarity with other works, using similarity detection software that is connected with the study information system of the university member;
6. I transfer to the UL – free of charge, non-exclusively, geographically and time-wise unlimited – the right of saving the work in the electronic form, the right of reproduction, as well as the right of making the written final work of studies available to the public on the World Wide Web via the Repository of the UL;
7. I give my consent to the publication of my personal data included in the written final work of studies and in this declaration, together with the publication of the written final work of studies;
8. I give my consent to the use of my birth date in COBISS record.

In Ljubljana, _____

Student's signature: _____

Abstract

UDC 519.61:658.5:648.525(043.2)

Serial No.: MAG II/518 E

Engineering design of impeller for vacuum cleaner motor from polymer material

Luis Linares Leyva

Keywords: FEM analysis
 plastic impeller
 polymer welding
 shaft bindings
 vacuum cleaner

Power of vacuum cleaners is in the last years limited with regulation (directive 2009/125/ES, EU regulation no. 666/2013). Smaller power of appliances reduce thermal and mechanical load level on impellers. The new circumstances have opened the possibility for designing an impeller from polymer material. An open technical issue is the connection between plastic impeller and the shaft. The connection between the impeller and shaft is loaded with generated forces due to inertia at each start acceleration and with centrifugal forces resulted from high speed of rotation. Various design solutions were prepared according to the design methodology and were evaluated afterwards. In the evaluation, the complex conditions of use and the validation test that required 15000 start/stop cycles of the vacuum cleaner motor, and the maximum rotation speed of the impeller up to 60000 rpm were considered. The appropriate polymer material and the design connection between the plastic impeller and the shaft was selected. In addition, since the impeller was made up of two pieces, the specific characteristics of the joining technology were evaluated and then selected. Finite element method was used to analyse different proposals. Additionally, the cost constraints and the possibilities for serial production were considered.

Razvoj rotorja sesalne enote iz polimernega materiala

Luis Linares Leyva

Keywords: MKE analize
plastični rotor
varjenje polimerov
gredne vezi
sesalna enota

Moč sesalnikov je v zadnjih letih omejena z regulativo (direktiva 2009/12/ES, uredba EU št. 666/2013). Manjše moči naprav zmanjšajo toplotno in mehansko stopnjo obremenitve na rotorju. Nove okoliščine so odprle možnost za konstrukcijo rotorja iz polimernega materiala. Odprt tehnični problem je vez med plastičnim rotorjem in gredjo. Povezava med rotorjem in gredjo je ob vsakem zagonu obremenjena s silami zaradi vztrajnosti in s centrifugalnimi silami, ki so posledica visoke hitrosti vrtenja. Različne rešitve so bile pripravljene v skladu z metodiko konstruiranja in so bile naknadno ovrednotene. Pri vrednotenju so bili upoštevani zahtevni pogoji uporabe in validacijski test, ki je zahteval 15000 ciklov zagonov/zaustavitev motorja sesalnika in največjo vrtilno frekvenco rotorja do 60000 vrt/min. Izbran je bil primeren polimerni material in vez med plastičnim rotorjem in gredjo. Za spajanje sestavnih delov rotorja so bile ocenjene značilnosti različnih tehnologij in najbolj primerna je bila izbrana. Metoda končnih elementov je bila uporabljena za analizo različnih rešitev. Poleg tega so bile upoštevane stroškovne omejitve in možnosti serijske proizvodnje.

Table of contents

| | |
|---------------------------------------------------------------------------|-----------|
| 1. Introduction | 1 |
| 1.1. Background | 1 |
| 1.2. Objectives | 2 |
| | |
| 2. Theoretical background and overview of literature..... | 3 |
| 2.1. Background | 3 |
| 2.1.1. Technical issue..... | 5 |
| 2.2. Material selection..... | 6 |
| 2.2.1. Tested materials | 7 |
| 2.2.2. New study of materials | 8 |
| 2.2.2.1. CES EduPack 2017..... | 8 |
| 2.3. Joining technologies between the parts of the impeller | 9 |
| 2.3.1. Tested joining technologies | 9 |
| 2.3.1.1. Heat welding..... | 10 |
| 2.3.1.2. Infrared welding..... | 11 |
| 2.3.1.3. Ultrasonic welding..... | 12 |
| 2.3.1.4. Tested technologies results | 13 |
| 2.3.2. Other joining technologies..... | 14 |
| 2.3.2.1. Vibration welding | 14 |
| 2.3.2.2. Laser welding..... | 16 |
| 2.4. Design of the impeller | 18 |
| 2.5. Joining technologies between the shaft and the impeller | 18 |
| 2.5.1. Adhesive bonding | 19 |
| 2.5.2. Laser | 19 |
| 2.5.3. Inserts..... | 19 |
| 2.5.4. New hub design | 20 |
| | |
| 3. Methodology | 23 |
| 3.1. First steps | 23 |
| 3.1.1. Study of new materials | 23 |
| 3.1.2. Design | 28 |
| 3.1.2.1. External design | 29 |
| 3.1.2.2. Internal design | 39 |

| | |
|---------------------------------------------------------------|-----------|
| 3.2. Practical section..... | 51 |
| 3.2.1. Simulations to select the material..... | 51 |
| 3.2.2. Simulations to select the external design..... | 56 |
| 3.2.3. Simulations to select the internal design | 59 |
| | |
| 4. Results | 61 |
| 4.1. Material selection | 61 |
| 4.2. Design of the impeller | 64 |
| 4.2.1. External design | 64 |
| 4.2.2. Internal design | 66 |
| | |
| 5. Discussion | 69 |
| 5.1. Material..... | 69 |
| 5.2. Joining method between parts of the impeller..... | 71 |
| 5.3. Engineering design | 72 |
| 5.4. Joining method between shaft and impeller | 73 |
| | |
| 6. Conclusions..... | 77 |
| | |
| 7. Bibliography | 79 |

List of figures

| | |
|------------------------------------------------------------------------------|----|
| Figure 1.1: Rendering of a plastic impeller for a vacuum cleaner motor..... | 1 |
| Figure 2.1: Vacuum cleaner basic structure [2] | 4 |
| Figure 2.2: Theoretical basic design of the impeller [3] | 5 |
| Figure 2.3: Overall view of the issue | 6 |
| Figure 2.4: Heat welding process [1] | 11 |
| Figure 2.5: Ultrasonic cold forming [9] | 13 |
| Figure 2.6: Adhesive force [1] | 14 |
| Figure 2.7: Linear vibration welding machinery [9] | 16 |
| Figure 2.8: Laser welding in the automotive industry [11] | 17 |
| Figure 2.9: Cross-section of a plastic impeller [1] | 18 |
| Figure 2.10: Main objectives in section 2.5 | 19 |
| Figure 2.11: Enlarged exploded view of the hub of the impeller [14] | 20 |
| Figure 2.12: Top plan view of an impeller for the blower [14]..... | 21 |
| Figure 3.1: CES EduPack 2017. First steps [6]..... | 24 |
| Figure 3.2: Young's modulus (GPa) vs. Price (€/kg) [6] | 25 |
| Figure 3.3: Elastic limit (MPa) vs. Price (€/kg) [6]..... | 26 |
| Figure 3.4: Tensile strength (MPa) vs. Density (kg/m ³) [6]..... | 26 |
| Figure 3.5: Elastic limit (MPa) vs. Density (kg/m ³) [6]..... | 27 |
| Figure 3.6: Overall view of material selection | 28 |
| Figure 3.7: Cross-section of a plastic impeller with tolerances [1]..... | 29 |
| Figure 3.8: Impeller cover. Step 1 | 30 |
| Figure 3.9: Impeller cover. Step 2..... | 30 |
| Figure 3.10: Impeller cover. Step 3..... | 31 |
| Figure 3.11: Impeller cover. Step 4..... | 31 |
| Figure 3.12: Impeller blades. Step 1 | 32 |
| Figure 3.13: Impeller blades. Step 2 | 32 |
| Figure 3.14: Impeller blades. Step 3 | 33 |
| Figure 3.15: Impeller blades. Step 4 | 33 |
| Figure 3.16: Impeller blades. Step 5 | 34 |
| Figure 3.17: Impeller blades. Step 6 | 34 |
| Figure 3.18: Blade sketch..... | 35 |
| Figure 3.19: Impeller blades. Step 7 | 35 |
| Figure 3.20: Impeller blades. Step 8 | 36 |
| Figure 3.21: Approximate model of an impeller | 36 |
| Figure 3.22: Revolve cut sketch for IBS2 | 41 |
| Figure 3.23: Cross-section of the Impeller blades with shaft. Step 1 | 42 |
| Figure 3.24: Impeller blades with shaft. Step 2..... | 42 |
| Figure 3.25: Impeller blades with shaft. Step 3..... | 43 |

| | |
|------------------------------------------------------------------------------------------|----|
| Figure 3.26: Shaft for IBS1. Step 1 | 43 |
| Figure 3.27: Sketch of one of the split lines..... | 44 |
| Figure 3.28: Shaft for IBS1. Step 2 | 45 |
| Figure 3.29: Shaft for IBS1. Step 3 | 45 |
| Figure 3.30: Coincidence of faces relation..... | 46 |
| Figure 3.31: AS1 (assembly with shaft 1)..... | 46 |
| Figure 3.32: Revolve cut sketch for S2 | 47 |
| Figure 3.33: Shaft for IBS2. Step 2 | 48 |
| Figure 3.34: Shaft for IBS2. Step 3 | 48 |
| Figure 3.35: Shaft for IBS2. Step 4 | 49 |
| Figure 3.36: Shaft for IBS2. Step 5 | 49 |
| Figure 3.37: AS2 (assembly with shaft 2)..... | 50 |
| Figure 3.38: Overall view of internal design..... | 51 |
| Figure 3.39: Project schematic in the starting point [16] | 52 |
| Figure 3.40: Cylindrical Coordinate System..... | 54 |
| Figure 3.41: PA6 (50% glass fiber). Tensile modulus (MPa) vs. Temperature (°C) [17]..... | 55 |
| Figure 3.42: Overall view of material simulations..... | 56 |
| Figure 3.43: Environment conditions for external design simulations..... | 57 |
| Figure 3.44: Project tree for the external design [16]..... | 58 |
| Figure 3.45: Overall view of external design simulations..... | 58 |
| Figure 3.46: Environment conditions for internal design simulations | 59 |
| Figure 3.47: Overall view of internal design simulations | 60 |
| Figure 4.1: Minimum and maximum points in the approximate model [16] | 63 |
| Figure 4.2: Minimum and maximum points in the real model [16] | 64 |
| Figure 4.3: Vibration modes in AS1 [16]..... | 66 |
| Figure 4.4: Vibration movement in Mode 2 [16] | 67 |
| Figure 4.5: Vibration movement in Mode 3 [16] | 67 |
| Figure 5.1: Overall view of section 5.1 and 5.2 | 72 |
| Figure 5.2: Overall view of section 5.3 | 73 |
| Figure 5.3: Overall view of section 5.4 | 76 |

List of tables

| | |
|------------------------------------------------------------------------------------------------------------------|----|
| Table 1.1: Boundary conditions [1]..... | 2 |
| Table 2.1: Typical values for strength-to-weight and stiffness-to-weight ratios for different materials [5]..... | 7 |
| Table 2.2: Already tested materials [1] | 7 |
| Table 2.3: CES EduPack 2017. Levels of database [6]..... | 9 |
| Table 2.4: The three tested joining technologies [1] | 10 |
| Table 2.5: Impeller parts welding [1]..... | 13 |
| Table 3.1: Material criteria..... | 24 |
| Table 3.2: Six main options for handling materials at the end of a product's life [6]..... | 25 |
| Table 3.3: Material/Colour relationship for the new materials study [6] | 27 |
| Table 3.4: Material/Properties relationship for the new materials study [6] | 27 |
| Table 3.5: Materials [6]..... | 28 |
| Table 3.6: Design values for IC (Figure 3.7) | 37 |
| Table 3.7: Design values for IB (Figure 3.7) | 37 |
| Table 3.8: Moments of inertia of the assemblies [15]..... | 38 |
| Table 3.9: Overall view of the formation of assemblies for external design..... | 39 |
| Table 3.10: Design values for IBS (impeller blades with shaft) | 39 |
| Table 3.11: Overall view of the formation of assemblies for internal design | 50 |
| Table 3.12: Assigned properties to each material at 22 °C [6] | 53 |
| Table 3.13: Corresponding weight to each material [6]..... | 53 |
| Table 3.14: Assigned properties to each material at 120 °C..... | 55 |
| Table 4.1: Results for material simulations at 22 °C [16] | 61 |
| Table 4.2: Results for material simulations at 120 °C [16] | 62 |
| Table 4.3: Results for material simulations at 120 °C with the real impeller [16] | 63 |
| Table 4.4: Results for external design simulations [16]..... | 65 |
| Table 4.5: Generated torques | 65 |
| Table 4.6: Frequencies in modes 2 and 3 [16] | 66 |
| Table 5.1: Material prices [6]..... | 70 |
| Table 5.2: Example of standardization for materials | 70 |
| Table 5.3: Normalized values for each material..... | 70 |
| Table 5.4: New normalized values | 71 |
| Table 5.5: Normalized values for each external design | 72 |
| Table 5.6: External design properties (Figure 3.7)..... | 73 |
| Table 5.7: Ratio for each internal design | 74 |
| Table 5.8: Internal design properties (Figure 3.7)..... | 74 |
| Table 5.9: Morphological matrix of joining methods | 74 |
| Table 5.10: Criteria matrix of joining methods..... | 75 |

List of symbols used

| Symbol | Unit | Meaning |
|----------|---------------------|----------------------|
| E | GPa | Young's modulus |
| G | GPa | Shear modulus |
| I | Kg·m ² | Moment of inertia |
| K | GPa | Bulk modulus |
| k | N·m ⁻¹ | Spring rate |
| m | Kg | Mass |
| α | Rad·s ⁻² | Angular acceleration |
| τ | N·m | Torque |
| ν | | Poisson's ratio |
| ω | Rad·s ⁻¹ | Angular frequency |

List of acronyms used

| Acronym | Meaning |
|---------|-----------|
| PA | Polyamide |

1. Introduction

1.1. Background

This research project carried out between the Laboratory for Engineering Design – LECAD and the company DOMEL HOLDING d.d., is based on the development of a thermoplastic material impeller for a new generation of vacuum cleaner motors. It nevertheless starts from a similar project, in which a series of possible materials and manufacturing technologies have been previously studied.

Power of vacuum cleaners is in the last years limited with regulation (directive 2009/125/ES, EU Commission Regulation 666/2013). Smaller power of appliance reduces thermal and mechanical load level on impeller. New circumstances have opened technical possibilities of impeller design from polymer materials.

This project is expected to be a turning point, not only in the development of a new generation of vacuum cleaner motors, but also in other projects, where electrical power is limited and there is an existing possibility of manufacturing some parts with polymers, instead of other materials with an overall cost reduction and identical functionality.

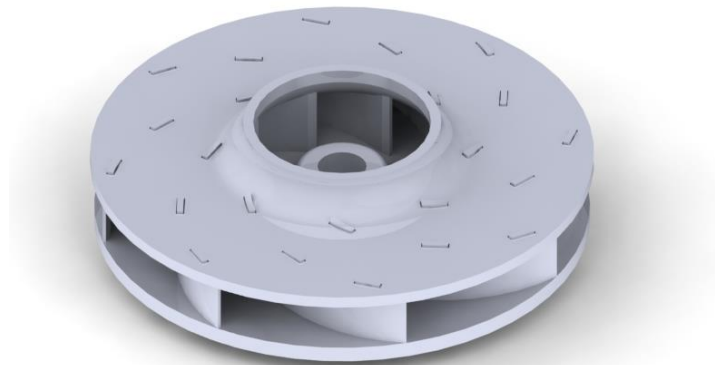


Figure 1.1: Rendering of a plastic impeller for a vacuum cleaner motor

It is possible to get an idea of the final shape of the impeller by rendering the Figure 1.1.

As some materials and technologies have already been tested in a similar project, the main problem is joining the impeller onto the shaft. Therefore, the different possibilities of this union will be studied, considering its advantages and disadvantages.

Furthermore, the working point and the maximum values in the boundary conditions shown in Table 1.1, must also be taken into account in this research project.

Table 1.1: Boundary conditions [1]

| Parameter | Working point | Maximum value |
|------------------------------------------|----------------|------------------------|
| Density | - | 1650 kg/m ³ |
| Impeller type | 2D | - |
| Impeller diameter | 60 mm | - |
| Impeller lifetime | 600 h | 3000 h |
| Input power | 400 W | 500 W |
| Material price | < 8 €/kg | - |
| Maximum air temperature | 50 °C | 70 °C |
| Rotational speed | 50000 rpm | 60000 rpm |
| Shaft temperature | 70 °C | 120 °C |
| Start/Stop cycles | > 15000 cycles | - |
| Percentage of water absorption after 24h | - | 4% |

1.2. Objectives

The overall objective of this master thesis has been to relate the theoretical knowledge, acquired in some subjects taught throughout the degree in industrial technology engineering and the industrial engineering master, in addition to the practical knowledge learned in the previous internship. So that with all this set of theoretical and practical experiences, it is desired to generate a series of ideas such as to solve the problem discussed in section 1.1.

The main objective of this project is to develop an impeller made of plastic of a vacuum cleaner motor, taking into account the selection of materials, the joining technology between the different parts of the impeller and finally, the connection technology between the impeller and the shaft.

The specific objective is to generate different options for the union between the impeller and the shaft.

2. Theoretical background and overview of literature

In this chapter we are going to introduce the reader what is going to be talked about throughout the project, starting with the problem and detailing what solutions can be applied to solve it.

2.1. Background

The basic operation of a vacuum cleaner consists of a high-revving motor, which turns a turbine (or impeller) inside a narrow chamber, thus producing the suction necessary to suck the air, and together with it, the dust that is desired to remove. That air flow is forced to pass through a filter element (can be paper, or a cloth bag), so that dirt is retained, leaving the clean air on the other side [2].

As we can see in Figure 2.1, the impeller is a small part of all the parts that make up the vacuum cleaner. Having the operation principle of a vacuum cleaner clear, the impeller is the part that is going to be discussed next.

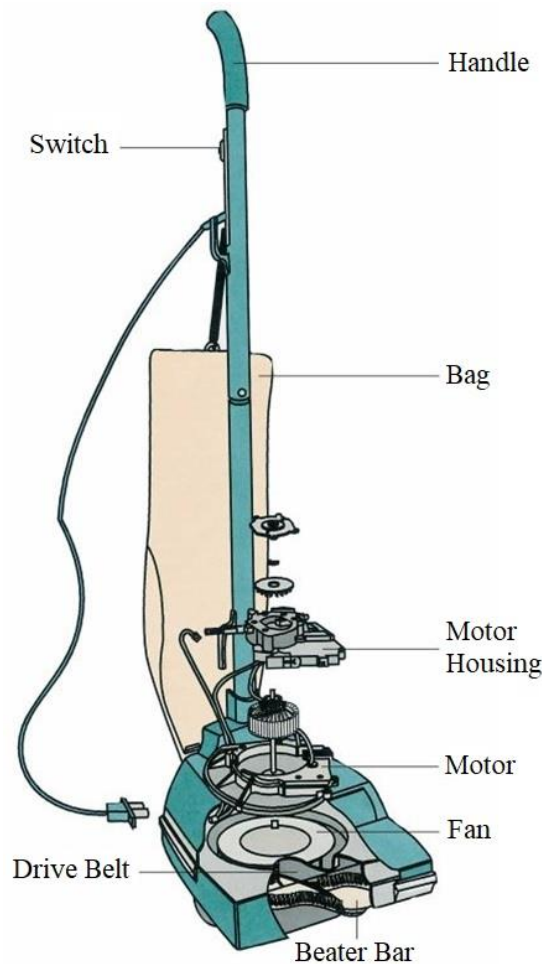


Figure 2.1: Vacuum cleaner basic structure [2]

An impeller is a rotor type located within a pipe or conduit and responsible for increasing (or decreasing in case of turbines) the flow and pressure of a fluid. It consists of a perpendicular disc to the axis of rotation, composed of curved blades in the opposite direction to the movement. The fluid enters the centre of the impeller and is dragged by the blades in a radial direction, as seen in Figure 2.2.

The impeller geometry is vital to achieve high hydraulic efficiency, and depending on the efforts to be supported and the aggressiveness of the medium to be propelled, the impeller can be made of a metallic alloy such as steel or aluminium, or of some polymer, such as polyamide [3].

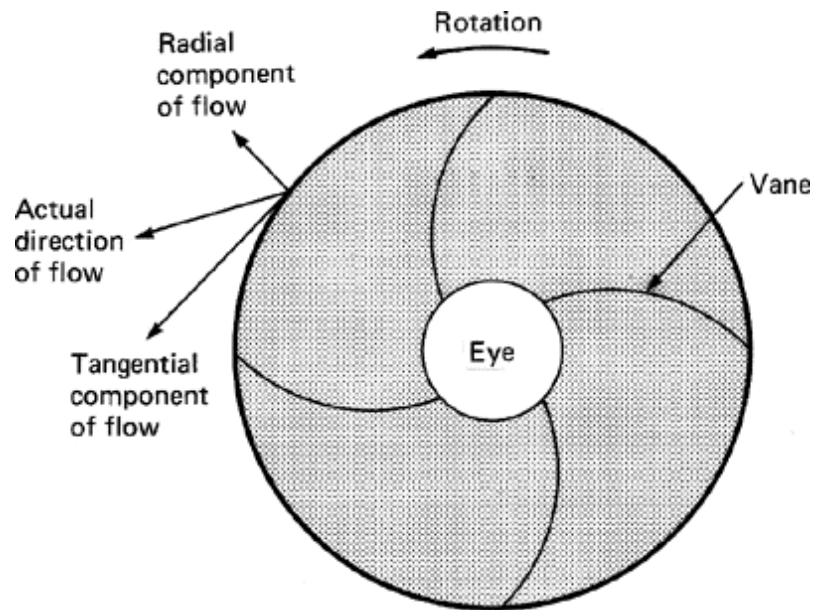


Figure 2.2: Theoretical basic design of the impeller [3]

2.1.1. Technical issue

Regarding the main objective of this project, to be able to develop an impeller made of plastic for a vacuum cleaner motor, a series of points are going to be written below that will help the reader to better understand the subject of the present technical issue.

First, we are going to do a brief explanation of the future design of the impeller, and the areas in which it can be variable. Second, we are going to talk about the materials for the impeller, of those that the company has carried out a study to arrive at the best solution, and those that we have proposed to study through the CES EduPack 2017 software. Later, we are going to talk about the technology studied for the union between the two parts of the impeller and, lastly, the technology of union between the impeller and the shaft.

As we have seen in [4], we are going to present the present project in a more global and visual way for the reader.

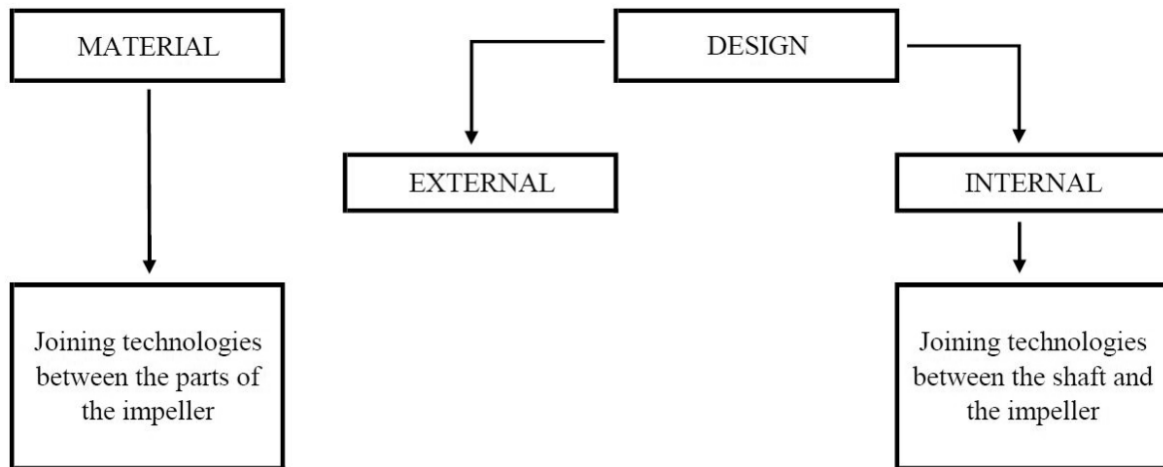


Figure 2.3: Overall view of the issue

It should be noted that of all the concepts seen in Figure 2.3, it has always been decided to make the option with the lowest possible cost

2.2. Material selection

In this section we are going to talk about the manufacturing material of the impeller, as well as ones already tested by the company. We are going to introduce how the study of new materials will be carried out, which is explained in the methodology section, in order to demonstrate that there may be better alternatives than the proposals, fulfilling with the boundary conditions of Table 1.1.

But before talking about the material types that have been studied, it is necessary to understand the classification of thermoplastics in the market, whether they are crystalline or amorphous. The appearance and development of plastic materials can be considered one of the great revolutions of the last century in terms of materials. The advances made in the production methods of these materials (which led to very affordable prices), together with their excellent characteristics meant that they were quickly accepted and used by the industry and construction sectors. The improvement of these characteristics was the next step in the attainment of materials increasingly suited to the productive needs, and the reinforcement with fibers of plastic materials is, without a doubt, the best example of this improvement.

Fibre-reinforced thermoplastics are more competitive than other types of composites or even metals, such as steel, aluminium or titanium alloys because they have better strength-to-weight and stiffness-to-weight ratios as we can see in Table 2.1 [5].

Table 2.1: Typical values for strength-to-weight and stiffness-to-weight ratios for different materials [5]

| Material | Strength/Weight (MPa/kgm ⁻³) | Stiffness/Weight (MPa/kgm ⁻³) |
|------------------|------------------------------------------|-------------------------------------------|
| Steel | 0,25 | 27 |
| Aluminium alloys | 0,20 | 26 |
| Titanium alloys | 0,20 | 25 |
| AS4/PEEK | 1,40 | 84 |
| IM6/epoxy | 2,20 | 128 |

In principle, both parts of the assembly will be of the same material, although it will not be shown to be in that way until later sections have not been reached.

2.2.1. Tested materials

We can see the studied materials by the company in Table 2.2.

Table 2.2: Already tested materials [1]

| Material | Tensile elasticity modulus E [GPa] | Tensile strength R _m [MPa] | Charpy unnotched/notched impact strength at 23 °C (dry) [kJ/m ²] | Deflection temperature [°C] | Water absorption after 24h [%] | Flexural fatigue strength at 10 ⁷ cycles [MPa] | Density [kg/m ³] |
|----------------------------------------------------------|------------------------------------|---------------------------------------|------------------------------------------------------------------------------|-----------------------------|--------------------------------|-----------------------------------------------------------|------------------------------|
| Amodel AS-4133 HS BK 324 (black) (PPA + 33% GF) | 11,7 | 172 | 67/11 | 294 | 0,29 | - | 1450 |
| Ultradur B 4300 G10 (black) (PBT + 50% GF) | 16,5 | 160 | 60/11 | 215 | 0,4 ... at saturation | - | 1730 |
| Nilamid AXP 146 01 black 0190 (PA66/6 + 60% GF) | 15 | 210 | 65/14 | 240 | 3,2 | - | 1660 |
| Grivory HTV-3H1 black 9205 (PA 6T/6I + 30% GF) | 11 | 170 | 50/7 | 280 | 3,5 ... at saturation | - | 1440 |
| Ixef 1022/9008 black (PARA + 50% GF) | 20 | 255 | 70/11 | 230 | 1,5 | 60 | 1640 |
| GrilonTSGL-40/4 black 9833 (PA 66 + PA 6 + 40% long GF) | 10 | 160 | 75/25 | 250 | 5,0 ... at saturation | - | 1450 |
| GrivoryGVL-5Hblack 9915 (PA 66 + PA 6 I/X + 50% long GF) | 17 | 230 | 95/30 | 255 | 4,0 ... at saturation | 53,3 | 1560 |
| Grivory HTV-5H1 black 9205 (PA 6T/6I + 50% GF) | 17,5 | 240 | 80/11 | 285 | 3,0 ... at saturation | 86,7 | 1650 |

| | | | | | | | |
|-----------------------------------------------------------|-----|-----|-------|-----|-----------------------|------------------------------|------|
| ZytelHTN51G45HSL BK083 (black) (PA 66 + PA6T/XT + 45% GF) | 15 | 230 | 90/11 | 265 | 3,6 ... at saturation | 98 at 10 ⁵ cycles | 1580 |
| LUVOCOM 1-8793/LGF (PA66 + 50% long GF) | 18 | 270 | 85/- | - | - | - | 1590 |
| Grivory XE 4101 (PA10T/X + 40% GF) | 13 | 175 | 85/10 | - | 2 | - | 1490 |
| Ultem 2300 (PEI + 30% GF) | 9,5 | 165 | 40/10 | - | 0,9 ... at saturation | - | 1510 |
| PEEK | 28 | 265 | 45/7 | - | 0,3 ... at saturation | - | 1400 |

It is desired to have a material density less than 1650 kg/m³, which provides adequate values of resistance to deformations due to the high speeds of rotation, and that the percentage of absorption of water after 24 hours is less than 4%.

As can be seen in the Table 2.2, the last five will be the potential thermoplastic materials for the final selection of the impeller material.

2.2.2. New study of materials

It is considered very convenient to carry out a new study for the materials selection, since the one mentioned in the previous section 2.2.1, was carried out in the company. The used methodology is going to be explained in section 3.1.1.

We want to give a new point of view in case it is possible to find a materials list that fulfil with all the imposed conditions, mentioned in previous sections, and that its price is more economical, that after all is what is desired when a materials study is performed.

For it, we are going to use CES EduPack 2017 software, described in the following subsection.

2.2.2.1. CES EduPack 2017

CES EduPack 2017 is a set of teaching resources that helps students learn more and better about the world of materials in engineering, design, science and sustainable development. The software shows in an interactive and visual way the latest news, resources and data on materials, sustainability and additive manufacturing.

CES EduPack 2017 software has three levels of database, as we can see in Table 2.3, and when it opens you are asked to choose one of them.

Table 2.3: CES EduPack 2017. Levels of database [6]

| | Coverage | Content |
|---------|----------------------------------------------------------------------------------------------------------------------------------------------------------------------------------------------------------|--------------------------------------------------------------------------------------------------------------------------------------------------------------------------------------------|
| Level 1 | Around 70 of the most widely used materials drawn from the classes: metals, polymers, ceramics, composites, foams, and natural materials. Around 70 of the most widely used processes | A description, an image of the material in a familiar product, typical applications, and limited data for mechanical, thermal, and electrical properties, using rankings where appropriate |
| Level 2 | Around 100 of the most widely used materials. Around 110 of the most commonly used processes | All the content of Level 1, supplemented by more extensive numerical data, design guidelines, ecological properties, and technical notes |
| Level 3 | The core database contains more than 3000 materials, including those in Levels 1 and 2. Specialist editions covering aerospace, polymers, architecture, bio-materials, and eco-design are also available | Extensive numerical data for all materials, allowing the full power of the CES selection system to be deployed |

There are several data tables at each level and the most important are: Materials, Shaping Processes, Joining Processes, and Surface Treatment.

Each of the three levels can be interrogated by:

- Browsing. Exploring the database and retrieving records via a hierarchical index.
- Searching. Finding information via a full-text search of records.
- Selection. Use of powerful selection engine to find records that meet an array of design criteria.



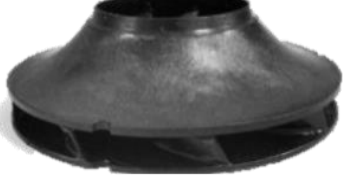
2.3. Joining technologies between the parts of the impeller

Our objective in this section is to achieve a union between the two parts of the impeller that fulfils the minimum of start/stop cycles, with the maximum temperature in service and with the maximum speed, that is, with the boundary conditions described above in Table 1.1. But there are a lot, as seen in [7], so we are going to see the most important for us.

2.3.1. Tested joining technologies

The three types of joining technologies between thermoplastics that have been studied and tested in the company will be presented below, although we can see a small result of them in Table 2.4, defining each one adding its advantages and disadvantages.

Table 2.4: The three tested joining technologies [1]

| | | |
|-----------------------------------------------------------------------------------|-----------------------------------------------------------------------------------|-------------------------------------------------------------------------------------|
|  |  |  |
| Heat welding | Infrared welding | Ultrasonic welding |

2.3.1.1. Heat welding

Heat welding, or thermal staking, is a thermoplastic welding technique that is characterized by raising the temperature of the plastic above its melting point to deform a bolt forming a head that mechanically blocks the two embedded components. A plastic bolt protrudes from a component fitted in the hole of the second component.

Care must be taken in providing heat so that it does not cause degradation in the material. The machinery cannot be turned on and off like other welding equipment, such as ultrasonic welding equipment, but instead they are very suitable for joining those materials with high percentages of fiberglass.

Among its great variety of characteristics, heat welding stands out for being versatile, fast and economical. It could even join plastics to other materials, such as metal for example, or even be able to join two varieties of thermoplastics. The fact is that in addition to being able to make this type of non-conventional joints, it stands out on other joining techniques not to use additional materials such as rivets and screws.

The best-known applications for this type of welding are usually found in the automotive industry, in medicine or in electronic products [8].

- Advantages [8]:
 - Compatible with most thermoplastics. Including the crystallines.
 - Easy assembly between both parts.
 - Greater bond strength of any welding process. The welding process creates permanent joints that cannot be opened without damaging them.
 - No additional materials. No additional materials are used such as inserts or screws, and the price is lower than other processes that use these types of fasteners.
 - Several joints can be made at the same time.
- Disadvantages [8]:
 - Accumulated melted plastic. Equipment must be cleaned before welding so as not to accumulate plastic before the operation.
 - Stakes can fail due to fatigue and impact.
 - Slow start process. To start the welding process, it must wait between 15 and 30 minutes for the matrix to warm up.

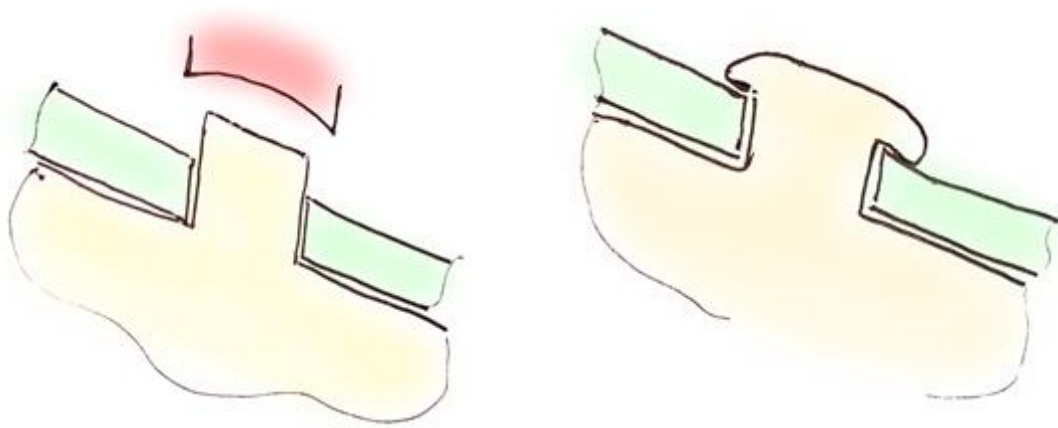


Figure 2.4: Heat welding process [1]

2.3.1.2. Infrared welding

Infrared welding does not require mechanical contact between the tool and the components to be welded. The result is a precise welding without applying any type of tension or heat on the welded surfaces. This system offers a very pleasant visual finish on components with complex geometries, large or small, so that the welding path can be programmed in three dimensions.

Care must be taken when joining materials reinforced with carbon fibre, considering the diffusion of heat in the part as they are good thermal conductors and, therefore, cool more quickly.

Infrared welding is used in many industrial processes such as joints in induction pipes, components for fans, tanks for brake fluid or for cleaning water in cars. Often these tubes and plastic containers are injection-moulded into half-shells that are then welded together [8].

- Advantages [8]:
 - Contactless heat transmission.
 - Ease of automation.
 - Maximum flexibility in joint design.
 - Minimum use of consumables. Infrared welding uses no additional materials such as inserts, screws or another kind of fasteners.
 - Very good surface quality.
- Disadvantages [8]:
 - Longer heating time. Longer heating times are needed to compensate for cooling during the changeover phase.
 - Machinery cost. It will depend on how sophisticated it is, but the costs are usually higher than the rest of the machinery of other welding processes.
 - Shape limitations.

2.3.1.3. Ultrasonic welding

Ultrasonic welding is the most indicated method if complex parts of injection-moulded thermoplastics must be joined, since it can be easily customized to adapt the exact specifications of the parts to be welded. This process is a good automated alternative to adhesive bonding, screws or snap-fit designs since it usually works with small parts.

It produces the local fusion of the plastic due to the absorption of the energy produced by the vibrations, and can be used for hard, soft and semi-crystalline plastics.

This type of welding has reached very advanced levels of technological development due to the increasing demands of plastic and electronic components in various industrial processes. In this sense it is possible to talk of robotized ultrasonic welding or multipoint ultrasonic welding. In the first case, it would be a technology for welding plastic materials by means of a sonotrode (vibrating tool) located at the end of the robot, equipped with a quick-change system of sonotrode that converts the system into multifunction; and in the second case, we would be talking about welding equipment equipped simultaneously with several ultrasonic generators capable of welding several points at the same time [8].

- Advantages [8]:
 - Easy assembly between both parts.
 - No additional materials. Ultrasonic welding uses no additional materials such as inserts, screws or another kind of fasteners.
 - Possibility to easily automate welding.
 - Several joints can occur at the same time. Additional parts can be joined between the welding parts as long as they do not affect this.

- Disadvantages [8]:
 - Compatible materials.
 - Machinery cost. The machinery cost is not very expensive, although it can increase a lot in case of microprocessor controlled machine. We can see the machinery in Figure 2.5.
 - Shape limitations. The maximum range in this welding process is 0,23 m x 0,3 m.
 - Size limitations.

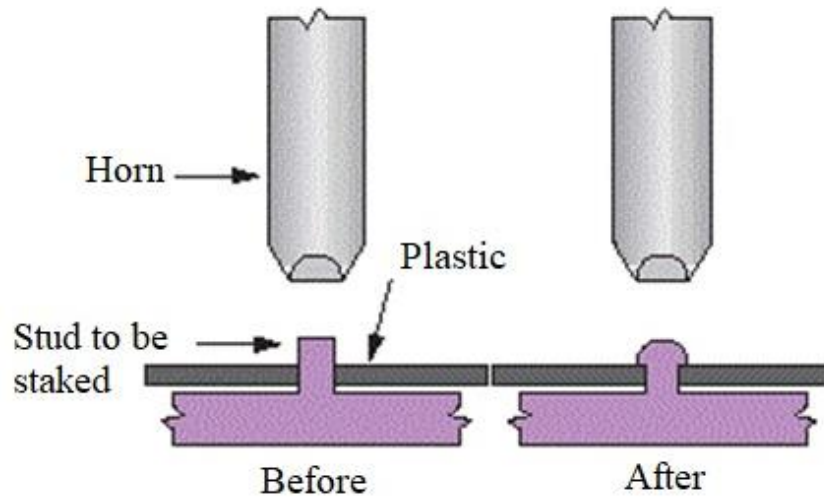


Figure 2.5: Ultrasonic cold forming [9]

2.3.1.4. Tested technologies results

The results of the different welding technologies applied by the company for the different proposed materials are shown in Table 2.5. In addition, the adhesive force for the same materials is also attached in Figure 2.6.

Table 2.5: Impeller parts welding [1]

| Material | Heat welding | Infrared welding | Ultrasonic welding |
|----------------------------------------------------------|----------------------|----------------------|----------------------|
| Amodel AS-4133 HS BK 324 (black) (PPA + 33% GF) | OK | Unable to weld | OK |
| Ultradur B 4300 G10 (black) (PBT + 50% GF) | NOT OK | NOT OK | OK |
| Nilamid AXP 146 01 black 0190 (PA66/6 + 60% GF) | NOT OK | Unable to weld | / |
| Grivory HTV-3H1 black 9205 (PA 6T/6I + 30% GF) | OK | Unable to weld | OK |
| Ixef 1022/9008 black (PARA + 50% GF) | Unable to make parts | Unable to make parts | Unable to make parts |
| GrilonTSGL-40/4 black 9833 (PA 66 + PA 6 + 40% long GF) | NOT OK | / | / |
| GrivoryGVL-5Hblack 9915 (PA 66 + PA 6 I/X + 50% long GF) | NOT OK | / | / |
| Grivory HTV-5H1 black 9205 (PA 6T/6I + 50% GF) | OK | Unable to weld | OK |

| | | | |
|-----------------------------------------------------------|----------------------|----------------|----|
| ZytelHTN51G45HSL BK083 (black) (PA 66 + PA6T/XT + 45% GF) | OK | Unable to weld | OK |
| LUVOCOM 1-8793/LGF (PA66 + 50% long GF) | Unable to make parts | / | / |
| Grivory XE 4101 (PA10T/X + 40% GF) | / | / | OK |
| Ultem 2300 (PEI + 30% GF) | / | / | OK |
| PEEK | / | / | OK |

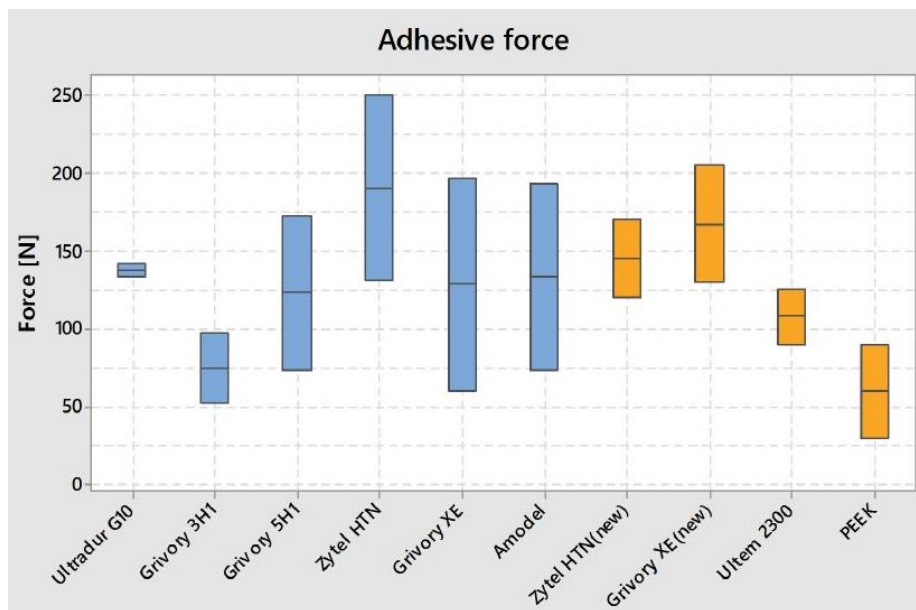


Figure 2.6: Adhesive force [1]

2.3.2. Other joining technologies

It is interesting to talk about other welding techniques to complement what has been described in previous sections, besides studying if it could be viable to use them. Therefore, we are going to explain two different techniques to the three previous ones, which are vibration welding and laser welding.

2.3.2.1. Vibration welding

Linear vibration welding consists of putting the materials in contact and pressed under pressure, moving one of the parts horizontally, and creating heat through the friction surface that melts, and welds the parts. In turn, the external force (as vibrations), will be applied in a perpendicular direction to the pressure load.

If we compare linear vibration welding with ultrasonic welding, we can say that the first is horizontal with frequencies between 120 and 300 Hz, while ultrasonic welding is vertical, with frequencies between 15000 and 72000 Hz. Normally the machinery manufacturers for both technologies are usually the same, and linear vibration welding handles higher ranges in terms of size for the welded parts, than ultrasonic welding.

Heat welding also finds similarities with linear vibration welding since the strength of the joints and the compatibilities with materials are approximately equivalent. However, although the cost of machinery is cheaper and has a greater range to manufacture shapes and sizes, it has a much longer cycle time, in addition to a higher fixation, energy and maintenance cost than linear vibration welding [8].

In principle all thermoplastics can be welded by this method, although it becomes quite useful in crystalline thermoplastics, which become very difficult to weld by ultrasound. Materials with low friction coefficients may require higher vibration frequencies for higher welding quality [10].

Linear vibration welding is applied mainly in the automotive industry and household appliances. Certain applications are, for example, dashboards, door panels, air inlet pipes or coffee makers among others.

- Advantages [8]:
 - Easy assembly between both parts.
 - No additional materials. Linear vibration welding uses no additional materials such as inserts, screws or another kind of fasteners.
 - Greater bond strength of any welding process. Linear vibration welding process creates permanent joints that cannot be opened without damaging them.
- Disadvantages [8]:
 - Compatible materials. Materials for linear vibration welding are limited to compatible thermoplastics.
 - Machinery cost. Are more expensive than heat welding equipment and cost considerably more than ultrasonic welders. We can see the machinery in Figure 2.7.
 - Shape limitations.

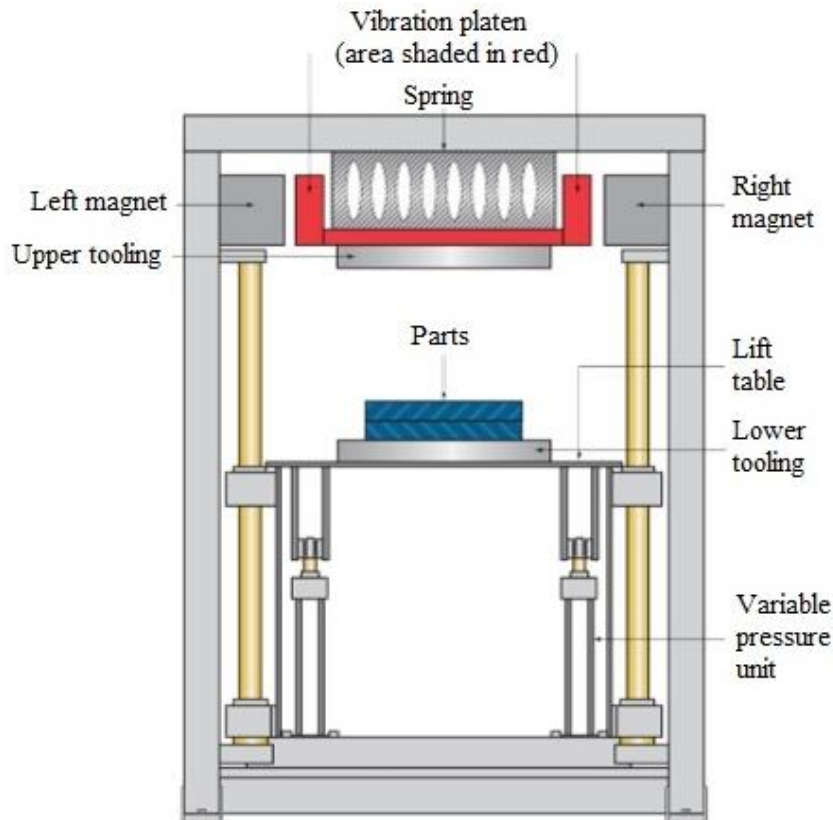


Figure 2.7: Linear vibration welding machinery [9]

2.3.2.2. Laser welding

Laser welding is a non-contact welding technique, used to join plastic or metal parts using a laser. From the concentrated heat of the beam, it allows the welder to achieve deep and close welds, as well as high welding rates.

The laser energy can also be used to melt plastic studs, which will eventually be pressed in order to weld it to the other part. It is necessary to consider in this union, the material of the two parts, since it is not possible to join certain thermoplastics.

Laser welding is the same as infrared welding using a laser as an energy source, the difference is that the second one uses halogen and parabolic lamps. Currently, the first has replaced the second for the surface welding. It is also very similar to hot plate welding, except that in this, a metal plate is used to heat the surface of the thermoplastic instead of a laser beam.

To be laser weldable, both thermoplastics must have a similar polymer structure and overlapping softening ranges. In addition, the thickness of the layer must be taken into account so as not to be restricted due to the limited laser energy transmittance. Although there are certain compatibilities between polymers for laser welding, they will not be included in this chapter [8].

We will choose the laser welding method in applications where high levels of precision are required, or those where surface marks are not tolerated. Laser welding is also used, when it is difficult to weld in holes that the machinery of other processes could not. Most of real applications are concentrated in the automotive sector and medical industries. One of the applications in automotive parts is showed in Figure 2.8.

- Advantages [8]:
 - Contactless heat transmission.
 - Good welding precision. The laser creates precision welds and no vibrations are transmitted to the welded part.
 - Contained heat-affected area. Due to the weld spot size.
 - No additional materials. Laser welding uses no additional materials such as inserts, screws or another kind of fasteners.
 - No special joint configuration. Reducing the cost of tooling.
- Disadvantages [8]:
 - Compatible materials. It is the main drawback of this welding process. It requires a thermoplastic material transparent to the laser light and the other thermoplastic that absorbs the laser energy.
 - Machinery cost. It will depend on how sophisticated it is, but the costs are usually higher than the rest of the machinery of other welding processes.
 - Shape limitations.



Figure 2.8: Laser welding in the automotive industry [11]

2.4. Design of the impeller

To make the design of the present impeller, two main considerations have been considered, to reduce the amount of secondary operations in the impeller, thus reducing the manufacturing cost, and having a good durability in the desired work environment. By manufacturing it in two parts, the cost in manufacturing and assembly is increased [12].

As already mentioned in section 2.1, the impeller geometry is essential to achieve a high hydraulic efficiency, but in this section only the theoretical part of the design will be commented, while in future sections, a more theoretical calculation of the possible change will be shown.

As can be seen in Figure 2.9, areas that are marked in red are subject to change, which means they may remain as they are or not. These changes will be effective depending on the material of manufacture, and the technologies of union between the parts of the impeller and the impeller with the shaft. All of them will be explained in the following sections.

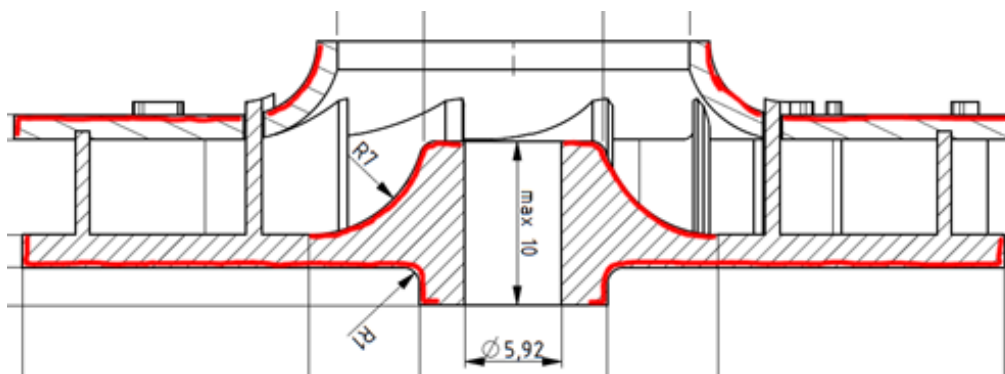


Figure 2.9: Cross-section of a plastic impeller [1]

2.5. Joining technologies between the shaft and the impeller

In recent years, plastic and metal joints have been made using adhesive bonding or riveting and clipping technologies. In fact, they are still being made today, although also through laser technology, it is not necessary to use additional materials or joining elements at the same time, so that it does not affect the quality of the final product.

Our objective in this section, will be to achieve a union that provides a good starting torque and that the movement is limited in the axial and radial direction, as we can see in Figure 2.10 and as was also intended in [13].



Figure 2.10: Main objectives in section 2.5

2.5.1. Adhesive bonding

In case of joining using an adhesive, before selecting it, it is necessary to take into account for what type of articulation/stresses the object will work, the distribution of efforts and the adequate preparation of the surface. Another important factor is the temperature at which it is going to work, and if it will support it. In any case, there are adhesives products of the mixture of two epoxies, which can work in a temperature range between -50 and 120 °C.

2.5.2. Laser

In case of using the laser as a joining method, first the area of the metal part involved in the joint, normally an insert, is subjected to a microtexturing process using a high-power laser. Next, the plastic part is placed on the metal part and the area is irradiated with a low power laser, so that the plastic melts, and at the same time by pressure, the fluid is forced to penetrate the holes in the preciously treated area.

The main advantages of this technology are a greater versatility, and the speed of the joining process compared to conventional processes, easy automation, a weight reduction in the final product since it is not necessary to add additional materials, lower risks of contamination of the joint, negligible disturbance of the properties of the materials involved and an excellent precision, since the area affected by heat is minimal [8].

2.5.3. Inserts

It is also possible to put the inserts without having to melt the plastic. One of these methods can be carried out in cold, using friction and some plastic deformation to be able to transfer the torque properly to the shaft. Another possible option is the moulding of the plastic impeller around the metal insert [8].

2.5.4. New hub design

There is another way of joining the shaft with the impeller, very different from those we talked about before, and that will be explained below.

As mentioned before, the techniques that have been used to join metal shafts to impellers made of thermoplastic materials have not been satisfactory due to their complexity and cost. The vibrations become very important during the movement, as well as the creep or plastic deformation due to the aging of the plastic.

So that a joint that is not subject to these problems will be needed and, it would be advisable that the fixation arrangement of the impeller is interchangeable, that is, that it can be removed from the driving motor if maintenance is necessary, or in case of break. As a last detail, it is also advisable to use the lowest number of parts in terms of the attachment between the shaft and the impeller.

The hub of the impeller includes three slots oriented axially, forming in it an internal structure with three cantilevers. We can see this design in Figure 2.11 and in Figure 2.12. One of them includes a flat surface on which the flat part of the shaft will be coupled. The other segments of the bundle include an internal transverse flange located in the hole cooperating with an annular slot in the driving shaft. A small flexible metal tube with a groove fits over the core preventing the segments of the beam from flexing outwards, thus ensuring the coupling.

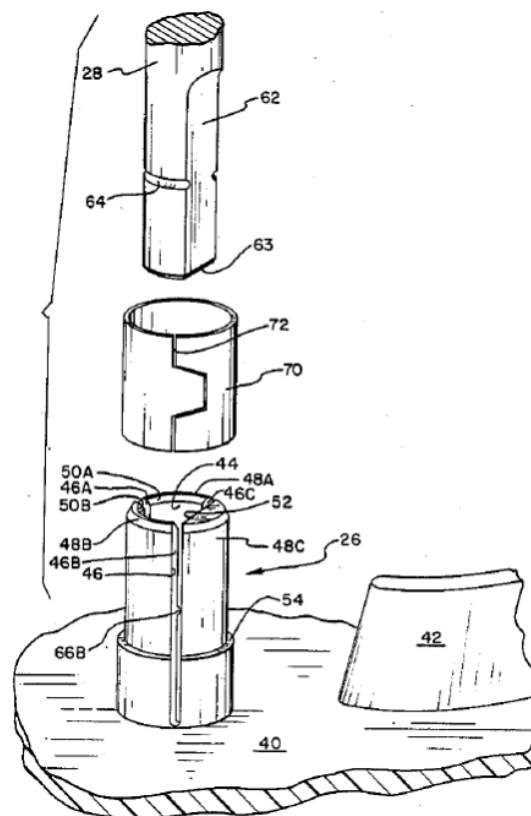


Figure 2.11: Enlarged exploded view of the hub of the impeller [14]

3. Methodology

This chapter focuses on the step by step explanations, of how the different sections of the proposed problem have been resolved, both for the first steps with the new materials and the design of the joint between the shaft and the impeller, as well as for the simulations in Ansys.

3.1. First steps

The first steps before making the calculations that determined the project final solution, went through a new study of materials with the help of the CES EduPack 2017 software, which detailed step by step how the final solution was reached. Finally, different design configurations were studied, approximated to what could be the real case, to choose the best ones after the simulations.

3.1.1. Study of new materials

When we started the CES EduPack 2017 software, the following window appeared, as we can see in Figure 3.1. In case it was a little detailed study of materials, we could choose any of the first levels, but given the project we are in, we chose Level 3, specialized in polymers.

Databases

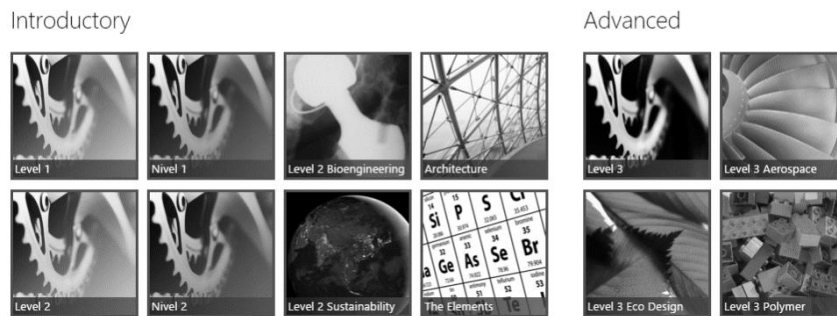


Figure 3.1: CES EduPack 2017. First steps [6]

Within the work interface, we clicked on the Chart/Select window to start a new study of materials. Once this was done, within the Selection Stages, we clicked on the Limit window to provide the software with the design criteria we wanted to fulfil in the list of 3968 available materials. We can see which parameters were chosen for the study in the following table.


Table 3.1: Material criteria

| | Minimum | Maximum |
|----------------------------------|---------|---------|
| Price | | |
| Price (€/kg) | - | 8 |
| Physical properties | | |
| Density (kg/m ³) | - | 1650 |
| Mechanical properties | | |
| Young's modulus (GPa) | 10 | - |
| Tensile strength (MPa) | 170 | - |
| Thermal properties | | |
| Melting point (°C) | 156 | - |
| Maximum service temperature (°C) | - | 120 |
| Absorption & Permeability | | |
| Water absorption @ 24 hours (%) | - | 1 |

The price per unit of weight was less than 8 kg, the density was less than 1650 kg/m³, the elasticity modulus (or Young's modulus) was higher than 10 GPa, the tensile strength was higher than 170 MPa, the melting point was higher than 156 °C applying a safety coefficient of 30% at the maximum temperature in service, which was lower than 120 °C, and the water absorption percentage after 24 hours was less than 1%.

In addition, it was possible to verify that none of the materials that managed to overcome the limits shown in Table 3.1, were recyclable, or at least they were not economically viable to recycle it. Anyway, all of them could be reprocessed in materials of lower quality (downcycle). The relative environmental impact of the six possible options for handling materials is summarized in Table 3.2.

Table 3.2: Six main options for handling materials at the end of a product's life [6]

| End of Life option | Description | Environmental burden |
|--------------------|------------------------------------------------------|-------------------------------------------------------------------------------------|
| Reuse | Extension of product life | Lowest |
| Re-engineer | Incorporation of re-engineered part into new product |  |
| Recycle | Reprocessing of material into primary supply chain | |
| Downcycle | Reprocessing into a lower grade material | |
| Combustion | Recovery of the calorific content of the material | |
| Landfill | Disposal of material | Highest |

Once the limits exposed, the software provided 8 materials that met the criteria of the 3968 available from the beginning. For a better selection, Figure 3.2, Figure 3.3, Figure 3.4 and Figure 3.5 will be shown in which we will be able to see the comparison between the Elasticity modulus (Young's modulus) vs. Price, between the Elastic limit vs. Price, between Tensile strength vs. Density and finally, between the Elastic limit vs. Density.

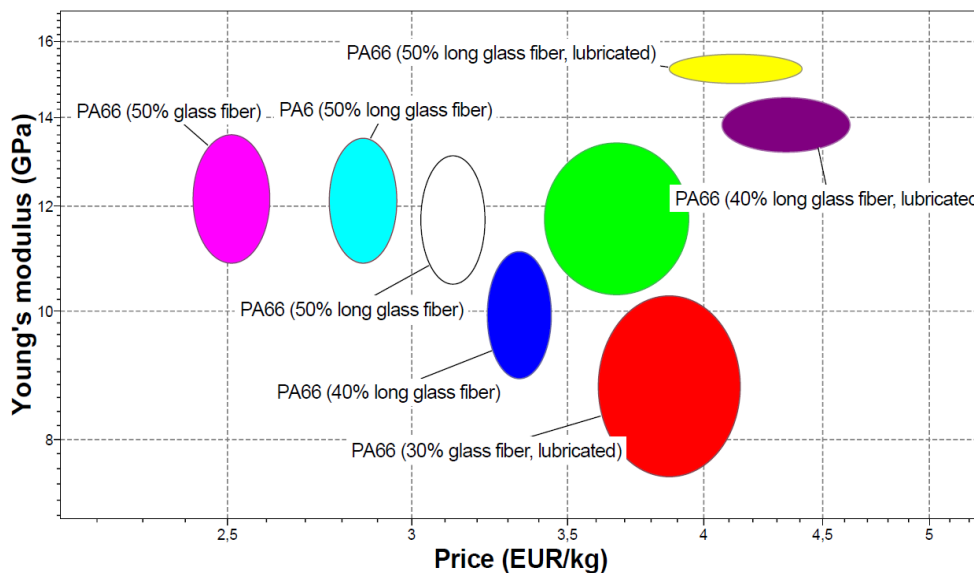


Figure 3.2: Young's modulus (GPa) vs. Price (€/kg) [6]

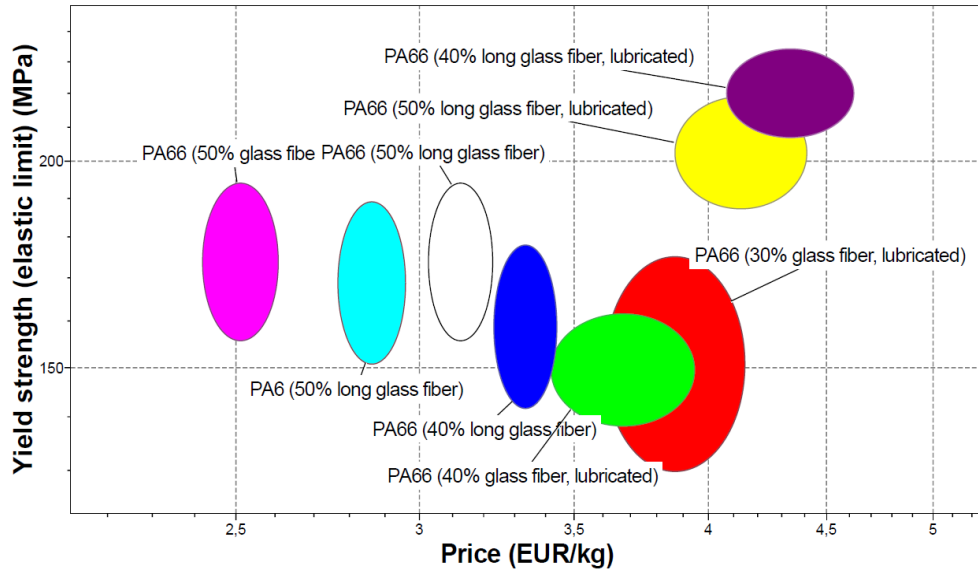


Figure 3.3: Elastic limit (MPa) vs. Price (€/kg) [6]

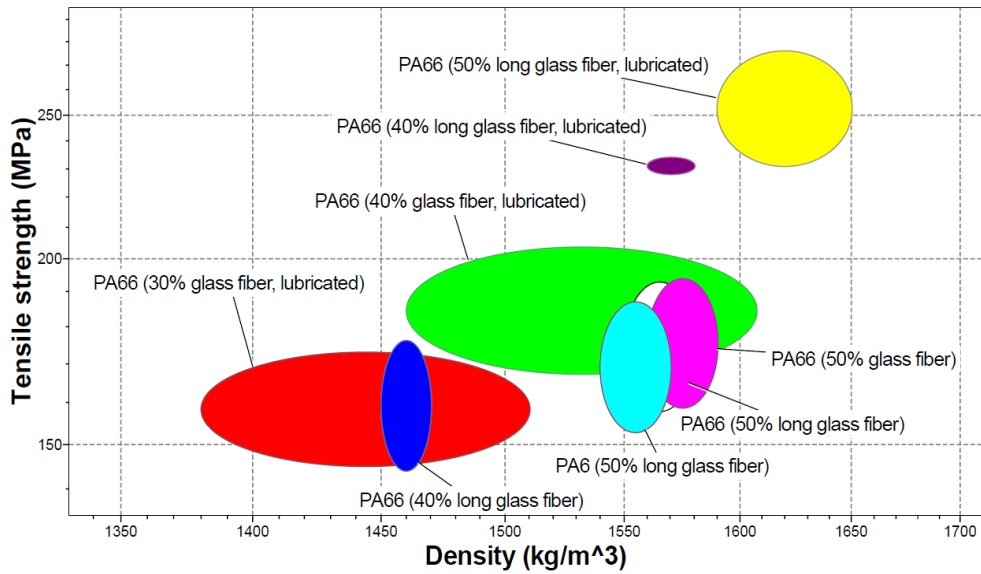


Figure 3.4: Tensile strength (MPa) vs. Density (kg/m³) [6]

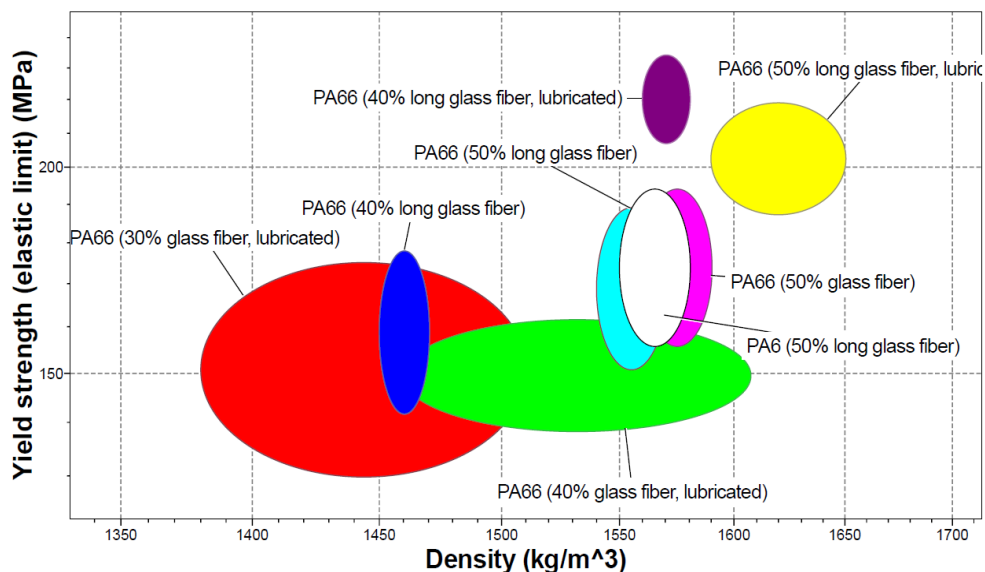


Figure 3.5: Elastic limit (MPa) vs. Density (kg/m^3) [6]

Next, we are going to see two tables. The first one, Table 3.3, in order to know the material/colour relationship and the next, Table 3.4, to show the properties extracted from the datasheet provided by CES EduPack 2017, of the eight selected materials.

Table 3.3: Material/Colour relationship for the new materials study [6]

| Material | Colour |
|--------------------------------|---------|
| PA6 (50% long GF) | Aqua |
| PA66 (30% GF, lubricated) | Red |
| PA66 (40% GF, lubricated) | Lime |
| PA66 (40% long GF) | Blue |
| PA66 (40% long GF, lubricated) | Purple |
| PA66 (50% GF) | Fuchsia |
| PA66 (50% long GF) | White |
| PA66 (50% long GF, lubricated) | Yellow |

Table 3.4: Material/Properties relationship for the new materials study [6]

| Material | Tensile elasticity modulus E [GPa] | Tensile strength Rm [MPa] | Deflection temperature 0,45MPa [$^{\circ}\text{C}$] | Water absorption after 24h [%] | Density [kg/m ³] | Price [€/kg] |
|---------------------------|------------------------------------|---------------------------|-------------------------------------------------------|--------------------------------|------------------------------|--------------|
| PA6 (50% long GF) | 10,9 - 13,5 | 153 - 187 | 215 - 264 | 0,93 - 1,5 | 1540 - 1570 | 2,77 - 2,95 |
| PA66 (30% GF, lubricated) | 7,51 - 10,3 | 145 - 173 | 238 - 265 | 0,55 - 1 | 1380 - 1510 | 3,61 - 4,15 |
| PA66 (40% GF, lubricated) | 10,3 - 13,4 | 168 - 204 | 245 - 270 | 0,5 - 1 | 1460 - 1610 | 3,42 - 3,94 |

| | | | | | | |
|--------------------------------|-------------|-----------|-----------|-------------|-------------|-------------|
| PA66 (40% long GF) | 8,9 – 11,1 | 144 - 176 | 229 - 281 | 0,37 - 0,6 | 1450 - 1470 | 3,23 – 3,44 |
| PA66 (40% long GF, lubricated) | 13,2 - 14,5 | 228 - 234 | 255 - 256 | 0,5 | 1560 - 1580 | 4,07 – 4,62 |
| PA66 (50% GF) | 10,9 - 13,6 | 159 - 194 | 225 - 276 | 0,46 - 0,74 | 1560 - 1590 | 2,42 – 2,51 |
| PA66 (50% long GF) | 10,5 - 13,1 | 158 - 193 | 260 - 314 | 0,46 - 0,74 | 1550 - 1580 | 3,03 – 3,22 |
| PA66 (50% long GF, lubricated) | 14,9 - 15,6 | 231 - 276 | 260 - 265 | 0,35 | 1590 - 1650 | 3,87 – 4,4 |

Therefore, the materials with which we worked from that moment are in Table 3.5 and the overall view of material selection can be seen in Figure 3.6.

Table 3.5: Materials [6]

| | |
|--------------------------------|--------------------------------|
| PA6 (50% long GF) | PA66 (30% GF, lubricated) |
| PA66 (40% GF, lubricated) | PA66 (40% long GF) |
| PA66 (40% long GF, lubricated) | PA66 (50% GF) |
| PA66 (50% long GF) | PA66 (50% long GF, lubricated) |

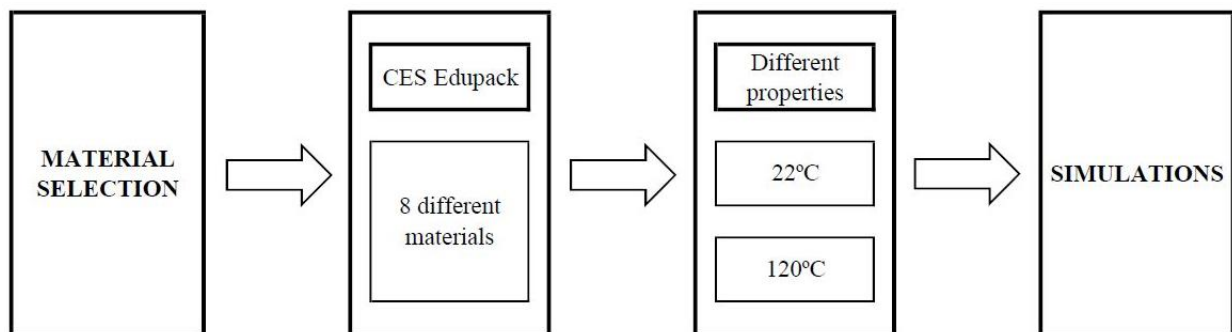


Figure 3.6: Overall view of material selection

3.1.2. Design

This section is divided into two parts, the first part is included within the external design while the second, is called as internal design, since it refers to the study of the joining technology between the shaft and the impeller in the central hole, as previously discussed in section 2.5.

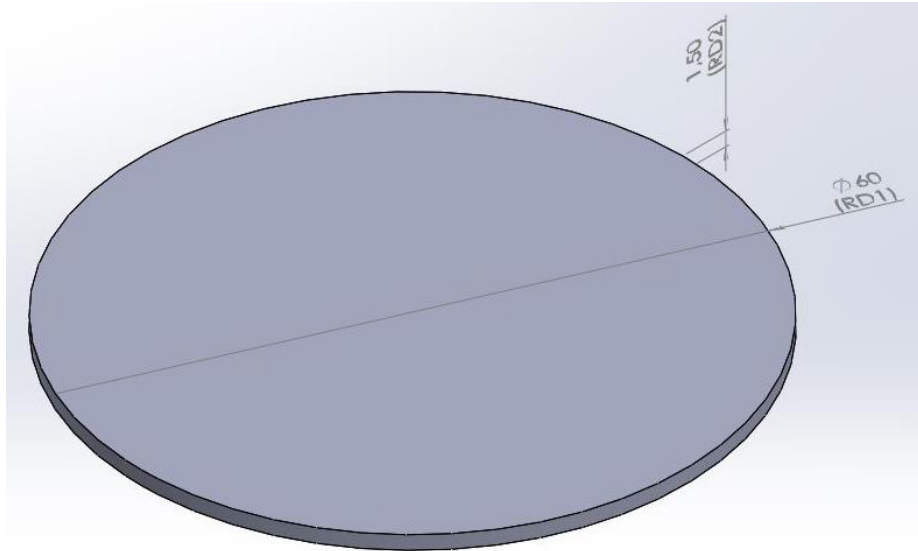


Figure 3.8: Impeller cover. Step 1

The next step to the Figure 3.8 was to create another circumference on the upper surface of the latter, with a diameter of 25 mm, number (6) in Figure 3.7, and a thickness of 4,5 mm, as we can see in Figure 3.9.

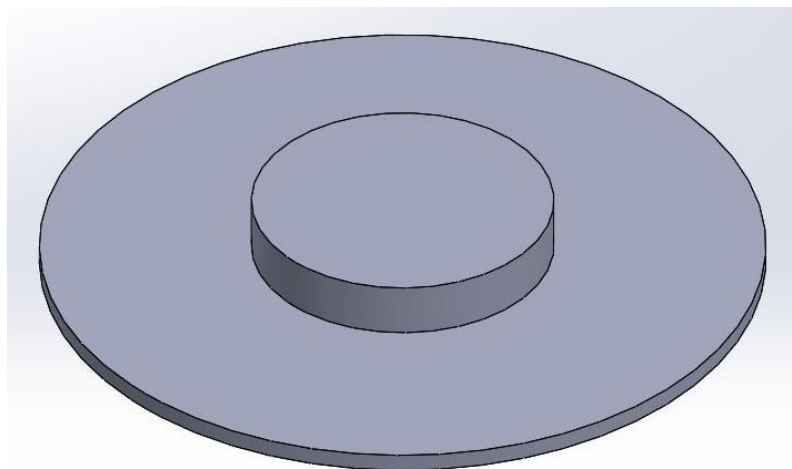


Figure 3.9: Impeller cover. Step 2

For the central hole, we draw another circumference of 21,5 mm on the upper face of the last extrusion. With the hole tool, we made a hole through the whole part, as seen in Figure 3.10.

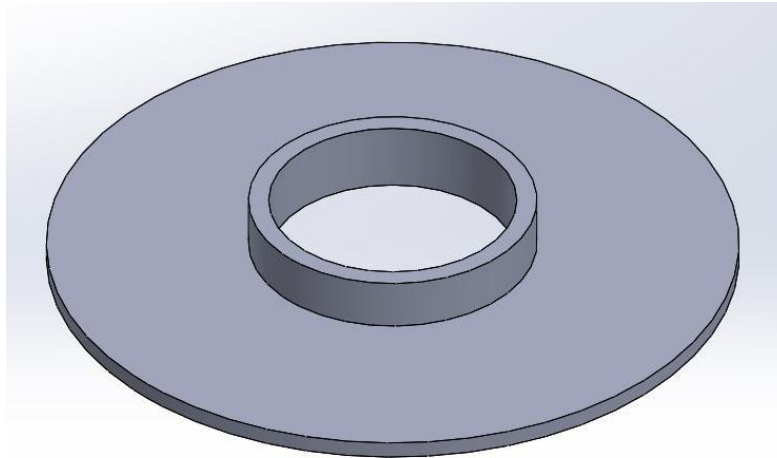


Figure 3.10: Impeller cover. Step 3

The last two operations were rounding profiles, one of 5 mm on the face that was extruded in step 2 and another of 5 mm inside of the hole, to avoid having internal stresses in a 90° angle corner (Figure 3.11).

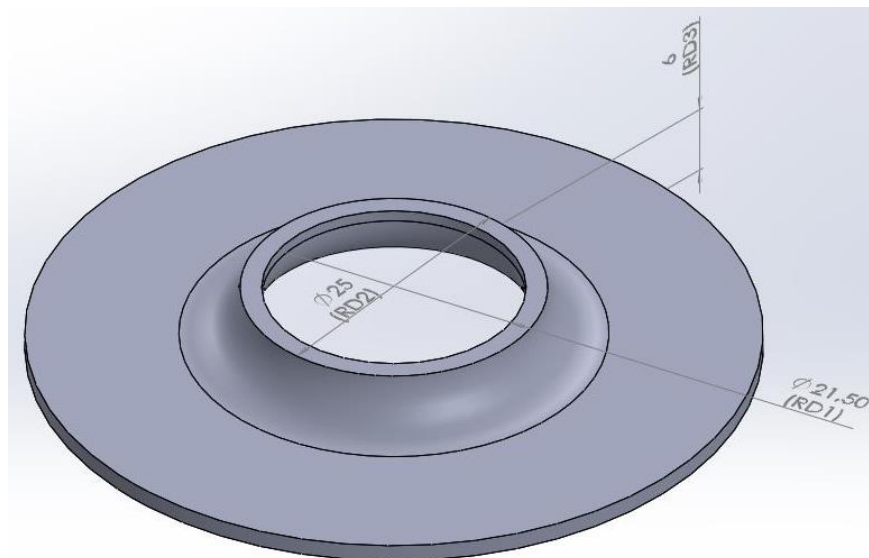


Figure 3.11: Impeller cover. Step 4

The second of the two parts was called IB1 as an abbreviation of impeller blades. It was also an approximation to the real model since the modelling of the blades was complex and had its study behind, so we tried to make it as close as possible.

We started by drawing a circumference of 11,5 mm in diameter, number (5) in Figure 3.7, with a thickness of 2,3 mm, since the sum of this thickness plus that of the circumference of the next step was to sum 4,3 mm in total, as seen in Figure 3.12.

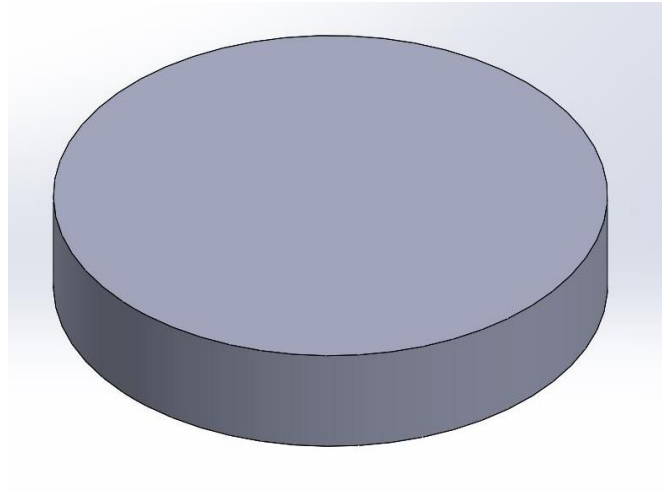


Figure 3.12: Impeller blades. Step 1

The next step therefore, in Figure 3.13, was to create another circumference on the upper surface of the previous extrusion, with a diameter of 60 mm and a thickness of 2 mm, number (3) in Figure 3.7.

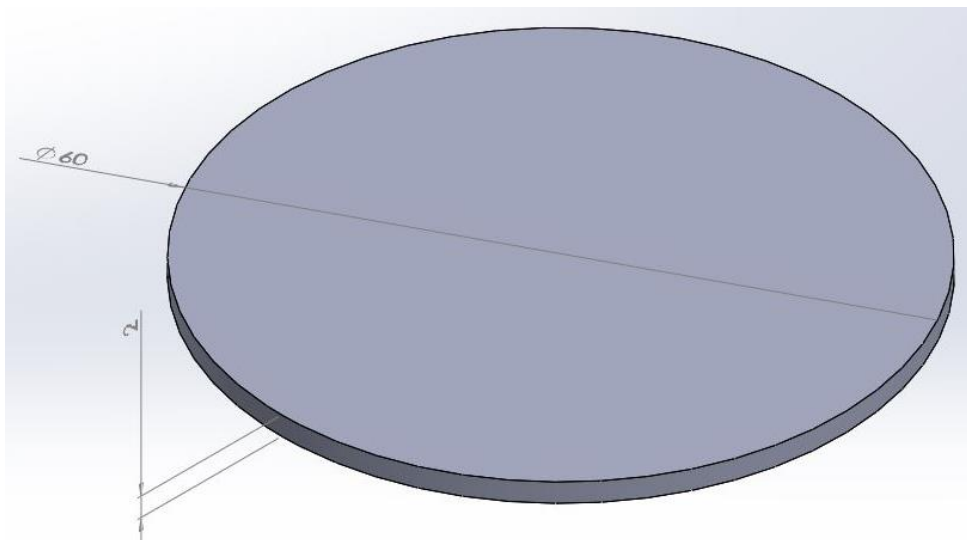


Figure 3.13: Impeller blades. Step 2

A sub-operation that was carried out was a rounded profile of 1 mm in the joining point between steps 1 and 2 of the impeller blades, as seen in Figure 3.14.

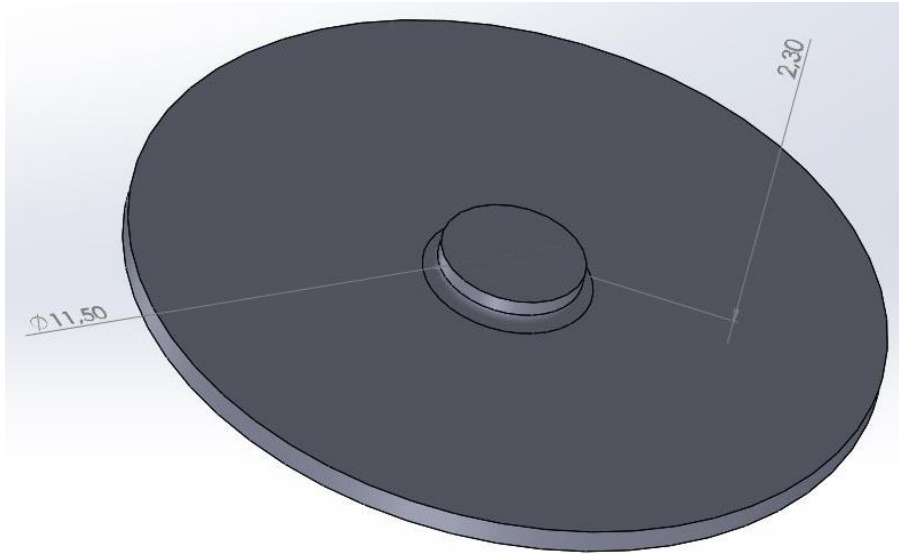


Figure 3.14: Impeller blades. Step 3

We made another circumference on the upper face of the step 2, this time with a diameter of 11 mm, number (1) of Figure 3.7, and 5,7 mm of thickness, as we can see in Figure 3.15.

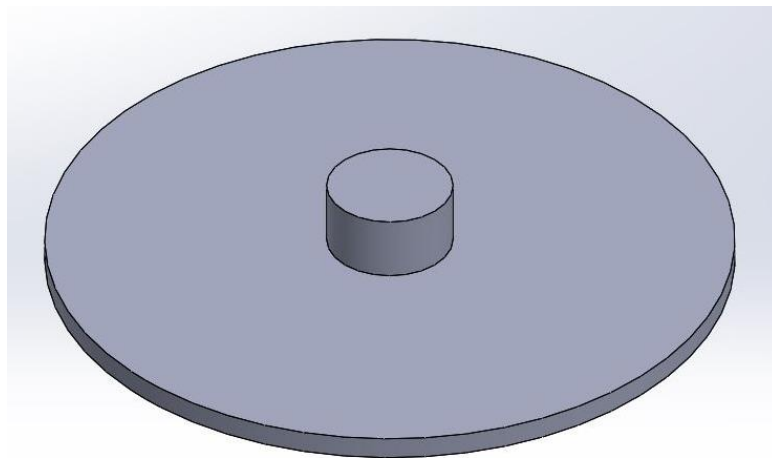


Figure 3.15: Impeller blades. Step 4

The next two sub-operations were two rounded profiles, one of 7 mm for the cylindrical face of the extrusion in step 4, and another of 0,5 mm for the apex of the extruded cylinder in the same step, as seen in Figure 3.16.

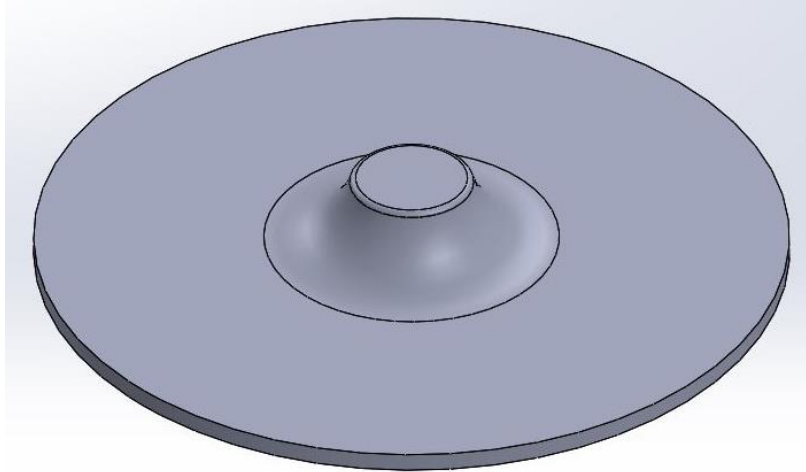


Figure 3.16: Impeller blades. Step 5

For the hole, we drew a circumference on the lower face of step 1, of 5,92 mm in diameter and a depth of 10 mm, number (4) in Figure 3.7, so it was a through hole, as we can see in Figure 3.17.

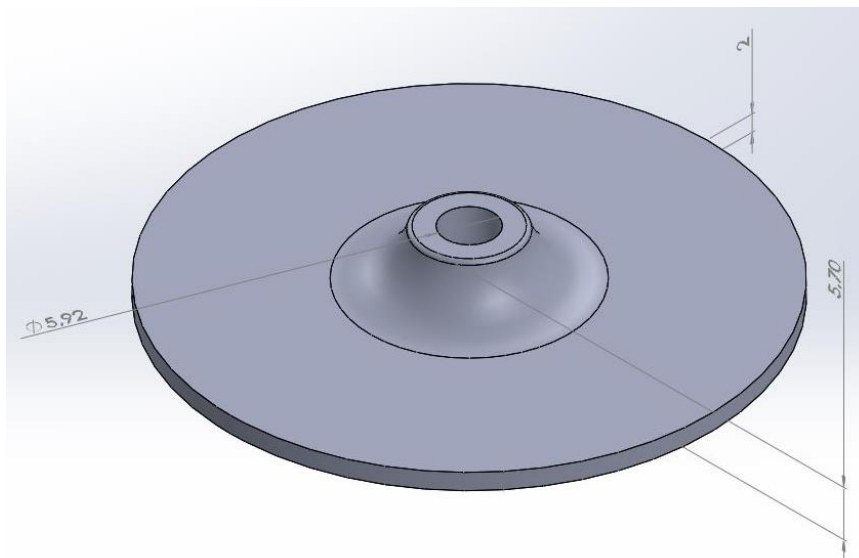


Figure 3.17: Impeller blades. Step 6

The next step was the most complicated, because it consisted in drawing one of the blades. To do this, two parallel circumferences of 22 mm in diameter were drawn on the upper face of the surface in step 2. They were joined at the ends as we can see in Figure 3.18, the excess lines were cut out and given to the polygon a thickness of 5,8 mm. The result is showed in Figure 3.19.

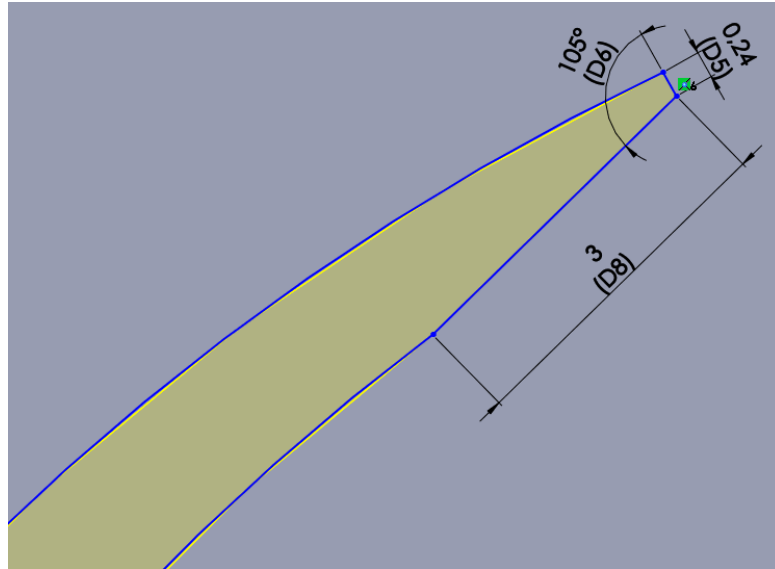


Figure 3.18: Blade sketch

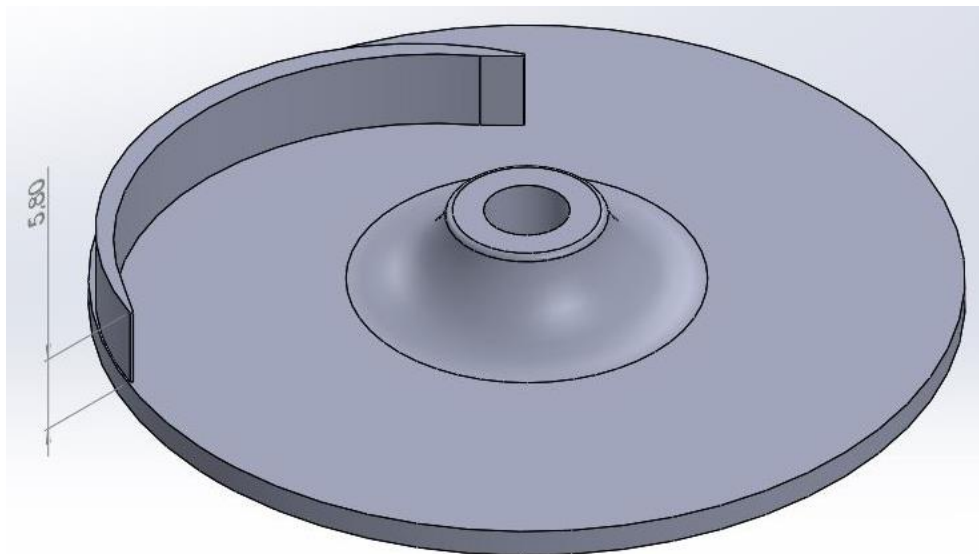


Figure 3.19: Impeller blades. Step 7

The last step, in Figure 3.20, was to make a circular matrix to create 7 more blades, equal to the first and around the entire circumference.

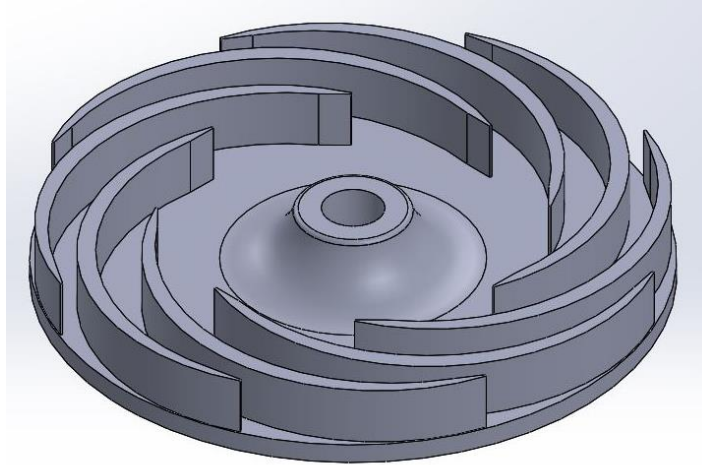


Figure 3.20: Impeller blades. Step 8

Modelled the two parts of the impeller, it was necessary to assemble them. So, in a new assembly file, called A1 (assembly 1) because it was an assembly and had nine more configurations, we imported both parts, and joined them as follows: first with a concentricity restriction, then with the coincidence of the same cutting plane, in this case it was a coincidence of the front plane, and finally, coincidence of the upper surface of the blades with the lower surface of the cover. The final result is in Figure 3.21.

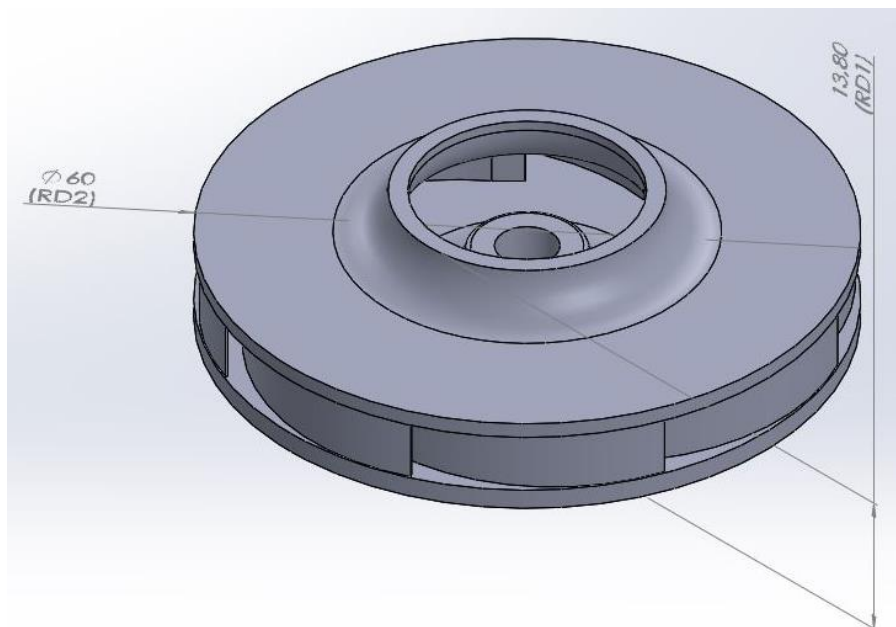


Figure 3.21: Approximate model of an impeller

At this point where we had an assembly with the measurements of Figure 3.7, we wanted to change the mentioned values between certain intervals, to offer different solutions and then

evaluate them to check which stresses and lower deformations were seen. To do this, we created a design table in SolidWorks, although this redirect us to an Excel table.

Starting with IC1, the values to change were (2) and (6), corresponding to the thickness of the cover and the largest diameter of the cover through which the air enters, respectively.

Although the values are not indicative for the results, because when using the RANDBETWEEN function of Excel every time we entered changed, it is important to see in Table 3.6 that there was a range of tolerances for each parameter, and that each configuration had its own value.

Table 3.6: Design values for IC (Figure 3.7)

| Impeller cover | (2) Cover thickness [mm] | (6) Cover hub diameter [mm] |
|----------------|--------------------------|-----------------------------|
| IC1 | 1,5 | 25,0 |
| Min | 1,0 | 23,5 |
| Max | 1,5 | 25,0 |
| IC2 | 1,0 | 23,8 |
| IC3 | 1,2 | 23,5 |
| IC4 | 1,0 | 24,9 |
| IC5 | 1,1 | 24,1 |
| IC6 | 1,2 | 23,6 |
| IC7 | 1,3 | 24,3 |
| IC8 | 1,4 | 24,0 |
| IC9 | 1,3 | 23,8 |
| IC10 | 1,4 | 23,6 |

And the same thing was done for IB (impeller blades) in Table 3.7.

Table 3.7: Design values for IB (Figure 3.7)

| Impeller blade | (5) Lower hub diameter [mm] | 4,3 – (3) | (3) Lower disc thickness [mm] | (1) Upper hub diameter [mm] |
|----------------|-----------------------------|-----------|-------------------------------|-----------------------------|
| IB1 | 11,5 | 2,3 | 2,0 | 11,0 |
| Min | 9,5 | 2,3 | 1,5 | 9,5 |
| Max | 11,5 | 2,8 | 2,0 | 11,0 |
| IB2 | 9,9 | 2,7 | 1,6 | 10,3 |
| IB3 | 9,6 | 2,8 | 1,5 | 9,5 |
| IB4 | 11,4 | 2,4 | 1,9 | 10,5 |
| IB5 | 10,4 | 2,4 | 1,9 | 10,1 |
| IB6 | 10,3 | 2,3 | 2,0 | 10,5 |
| IB7 | 9,7 | 2,8 | 1,5 | 9,5 |
| IB8 | 10,7 | 2,7 | 1,6 | 10,8 |
| IB9 | 11,3 | 2,5 | 1,8 | 10,4 |
| IB10 | 9,5 | 2,5 | 1,8 | 9,5 |

For the external design the hole depth for the shaft was not taken into account, which will be found in the next section. In addition, the second column on the left was a subtraction between the imposed measure of 4,3 mm between the upper part of the IB circumference and the base of IB, which depended on the thickness of the circumference.

To work with each configuration as if it were an independent part, a macro found online in a SolidWorks forum was used, which could extract each configuration and save it as a different file.

Finally, to have each assembly with its corresponding part numbers, that is, IC1 with IB1, it was assembled one by one as explained above in this same section.

The torque was also taken into account in order to know if the chosen design was the right one. According to the equation (3.1), we could calculate the torque by the multiplication of the moment of inertia on the axis of rotation by the angular acceleration.

$$\tau = I \cdot \alpha \quad (3.1)$$

The same angular acceleration, 2127,66 rev/s², or 13368,48 rad/s², was applied to each design configuration. This was known dividing the maximum speed of rotation (60000 rpm), between the time that the impeller passed from speed 0 rpm to maximum speed (0,47 seconds).

In terms of moments of inertia, they were obtained through the physical properties function of SolidWorks. We can see the values for each configuration in Table 3.8.

Table 3.8: Moments of inertia of the assemblies [15]

| Assembly | Inertia moment I [mg·m ²] |
|----------|---------------------------------------|
| A1 | 6,67 |
| A2 | 5,60 |
| A3 | 6,15 |
| A4 | 6,24 |
| A5 | 6,15 |
| A6 | 5,74 |
| A7 | 6,00 |
| A8 | 6,15 |
| A9 | 5,61 |
| A10 | 6,14 |

The results of the multiplication given by the equation (3.1), with the values from the Table 3.8, will be shown in section 4.2.1.

By way of summary, we have prepared Table 3.9 to better understand the concept of names for design.

Table 3.9: Overall view of the formation of assemblies for external design

| | | | | |
|------|---|------|---|-----|
| IB1 | + | IC1 | = | A1 |
| IB2 | + | IC2 | = | A2 |
| IB3 | + | IC3 | = | A3 |
| IB4 | + | IC4 | = | A4 |
| IB5 | + | IC5 | = | A5 |
| IB6 | + | IC6 | = | A6 |
| IB7 | + | IC7 | = | A7 |
| IB8 | + | IC8 | = | A8 |
| IB9 | + | IC9 | = | A9 |
| IB10 | + | IC10 | = | A10 |

3.1.2.2. Internal design

We are going to explain in this section how the internal design was made, or in other way, the design where the shaft is assembled. This has been defined on section 2.5 and now is going to be applied.

The first steps were the same as those discussed in the previous section, at least with respect to IB1, now called IBS1 with the “S” of shaft. The assembly will be discussed later, since there were other intermediate steps. The difference was that the number (4) of Figure 3.7 was the only one that was used in the SolidWorks and Excel design table, and was to create different depths between 7,5 and 9,7 mm in the hole where the shaft was. We can see them in Table 3.10.

Table 3.10: Design values for IBS (impeller blades with shaft)

| Part | (4) Hole depth [mm] |
|------|---------------------|
| IBS1 | 10 |
| Min | 7,5 |
| Max | 9,7 |
| IBS2 | 9,7 |
| IBS3 | 8,8 |
| IBS4 | 9,3 |
| IBS5 | 7,7 |
| IBS6 | 7,6 |

| | |
|-------|-----|
| IBS7 | 8,6 |
| IBS8 | 8,3 |
| IBS9 | 9,5 |
| IBS10 | 8,1 |

Other factors that were taken into account were that the part that acted as a cover, was the same in all assemblies since in this case, it was necessary to look at the internal design and not to the external changes, and IC1 was the common piece to all. The other factor is that the first case (IBS1) had a through hole, since we wanted to make a comparison of the design proposed by the company, making the calculations that are explained in the practical section.

Since we did not have to modify the part IBS1, we will move on to the methodology in the IBS2 design, since the subsequent pieces would be the same, changing only the depth values for the cut. And we say that we had to change the depth of the cut even though it was already done in each configuration, since to make the shape inside the slot where the shaft was assembled, we had to proceed to perform another type of operation that was not the hole. Therefore, the use that we gave to the configurations in this case, was only to calculate a random value for the depth.

The first step was to use the revolve cut tool. To do this, we chose the side view plane, although we could have used the front plane, and we made the sketch that we can see in Figure 3.22.

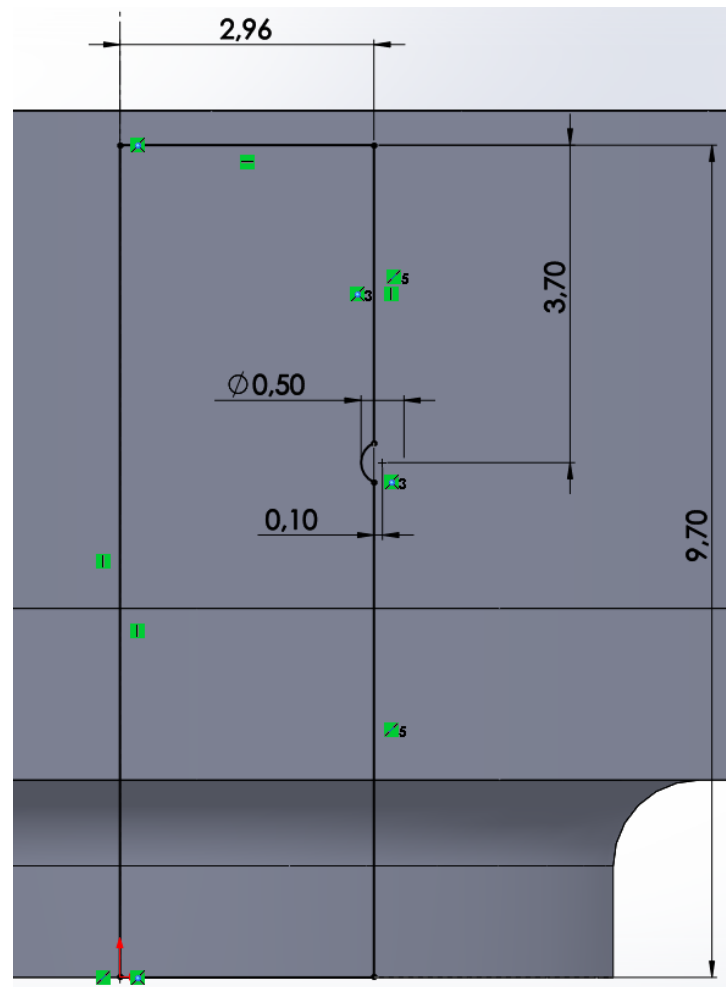


Figure 3.22: Revolve cut sketch for IBS2

As we can see in Figure 3.22, the axis of revolution was placed in the centre of the part, and 9,7 mm of depth was given as it marked the configuration. The 2,96 mm width of the hole was because the hole for the shaft was initially 5,92 mm in diameter, and we were doing half. Finally, and the most remarkable of the sketch, is the semicircle of 0,5 mm in diameter, displaced 0,1 mm to the right of the centre and 3,7 mm from the base of the hole. This is because the shape we saw in section 2.5 for the new configuration had a similar shape, with a ripple outward to a large extent from the inner cylinder. The result is shown in Figure 3.23.

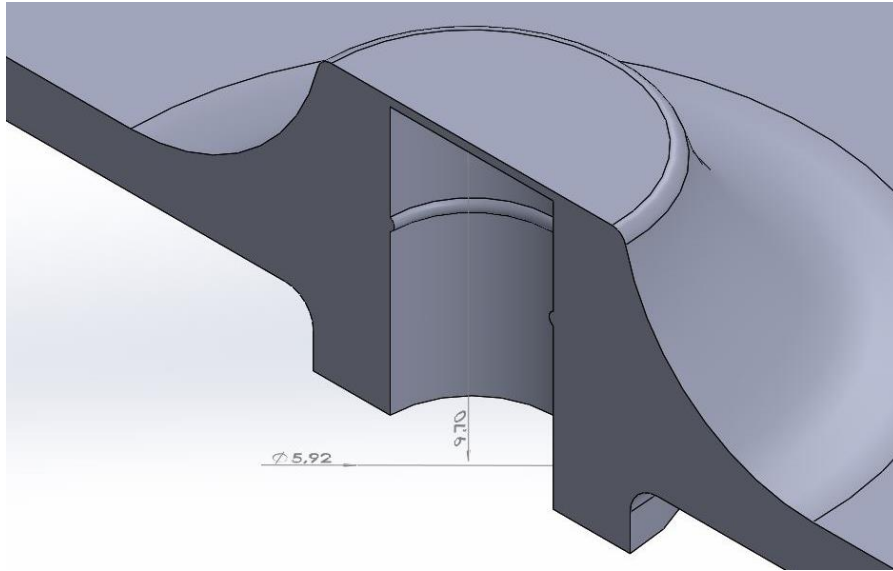


Figure 3.23: Cross-section of the Impeller blades with shaft. Step 1

The next step, in Figure 3.24, was to add the straight face inside the cylindrical hole, where the straight face of the shaft was placed when they were assembled. To do this, we made a sketch at the base of the hole and drew a circumference with the diameter of the hole. Next, we made a straight line that split the circumference at 2 mm from the centre of it. Finally, an extrusion was made with the distance of the depth marked by the configuration, in this case 9,7 mm.

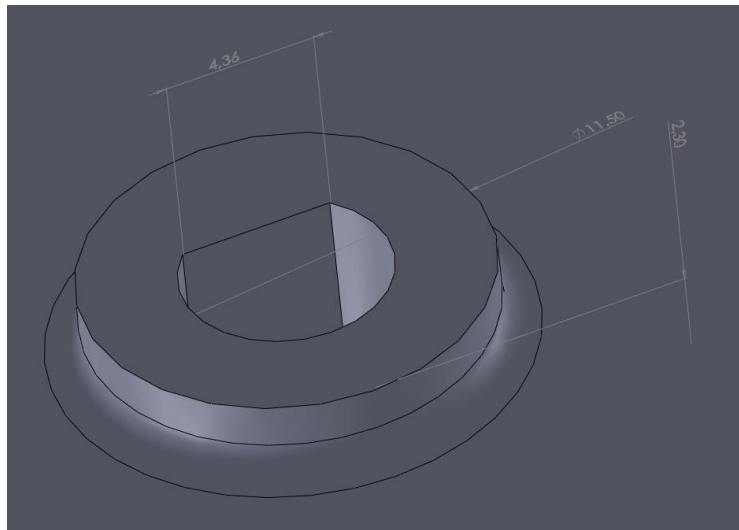


Figure 3.24: Impeller blades with shaft. Step 2

The last step, in Figure 3.25, was to make a chamfer of 0,3 mm at 45° to the outer vertices of the hole.

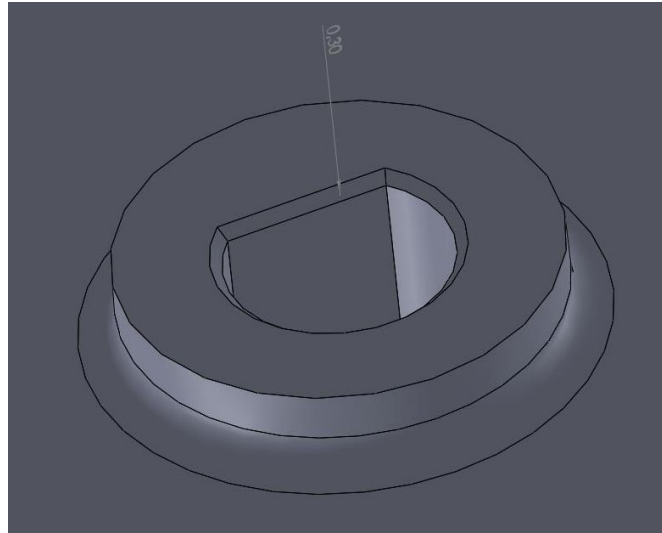


Figure 3.25: Impeller blades with shaft. Step 3

In this internal design section, the shaft design was also included, which was different for each of the configurations. Obviously, the shaft that was assembled with IBS1 had no flat face and was also the longest of all because it was presented like this in the real case, however, from IBS2 to IBS10, the shafts were similar although they changed certain values that we will discuss then.

The first step, for the shaft in IBS1, was to draw a circumference in the floor plan with a diameter of 5,92 mm, as seen in Figure 3.26. Then we used the extruding tool to convert the sketch into a cylinder of 95 mm in height.

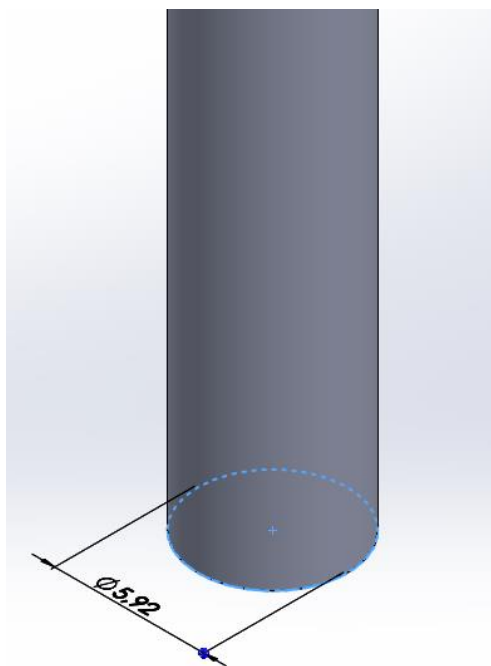


Figure 3.26: Shaft for IBS1. Step 1

The following was the most important step since, although it was not very useful in the design process, it was very useful in the simulations that are discussed in the practical section. What was done was to create two different split lines, since the shaft, besides supporting itself inside the impeller, was supported by two bearings.

So, to do this we made two different sketches on the front plane of the cylinder. All of them, were common to that there were two parallel lines that had their vertices on the outside face of the cylinder, as we can see in Figure 3.27.

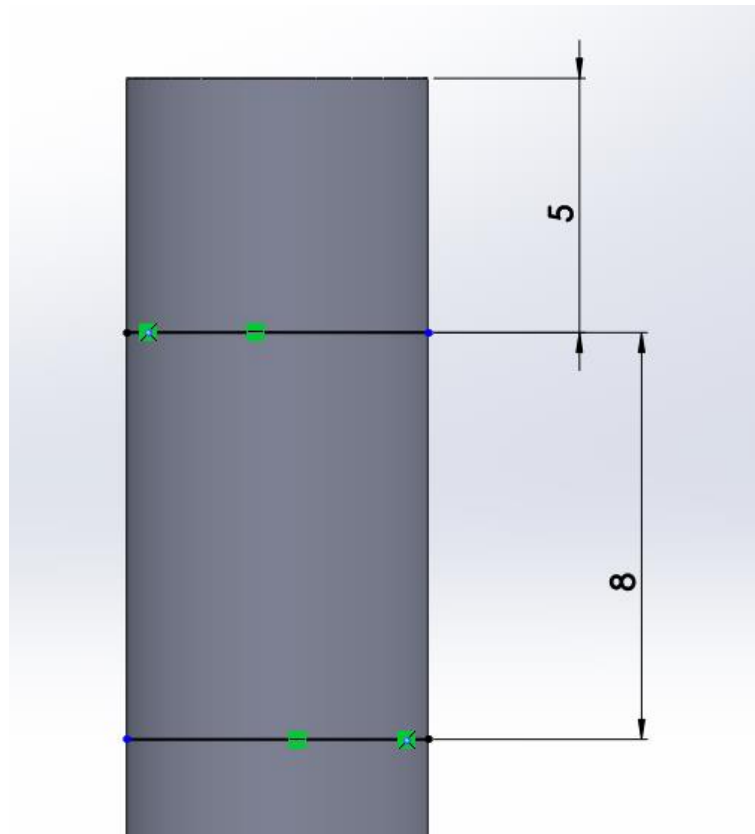


Figure 3.27: Sketch of one of the split lines

The only difference between the split lines was where they were placed. The first, corresponding to one of the bearings was placed 5 mm from the apex of the cylinder, and with 8 mm difference between the two parallel lines, while the other bearing was placed 16 mm from the opposite end to the first, with the same difference between lines, since the bearings were equal. The result is shown in Figure 3.28.



Figure 3.28: Shaft for IBS1. Step 2

The last step for this shaft was merely aesthetic, since two chamfers were made, one for each vertex at the ends, from 0,3 mm to 45°, as we can see in Figure 3.29.

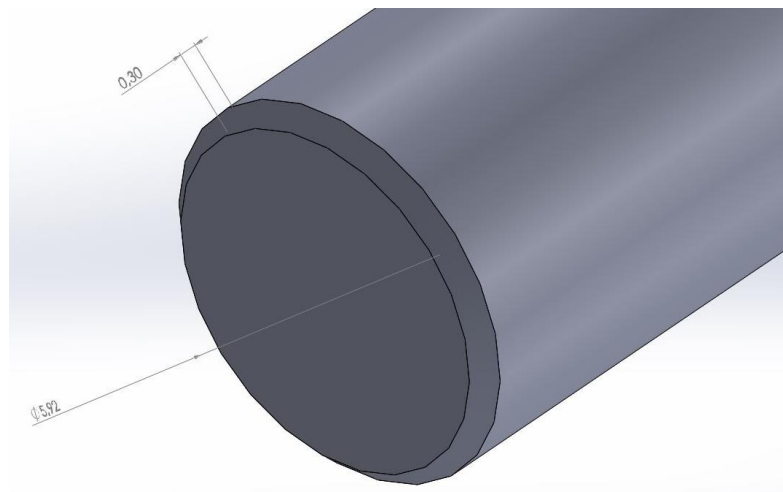


Figure 3.29: Shaft for IBS1. Step 3

The assembly consisted of three parts, IC1, IBS1 and S1. IC1 and IBS1 were assembled in the same way that we explained the assembly in section 3.1.2.1. However, we had in this case the shaft that was assembled to the set in the following way: with a concentricity relation with the hole of the impeller, with a coincidence relation of the top plane of IBS1, and finally with a relation of coincidence of faces to the distance of 6 mm, as we can see in Figure 3.30. The final result is showed in Figure 3.31.

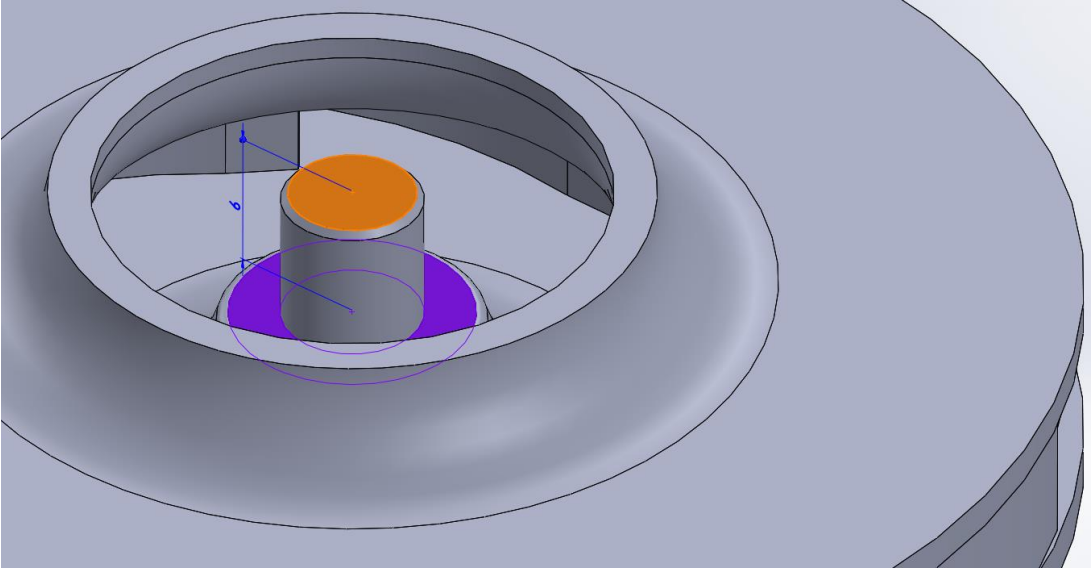


Figure 3.30: Coincidence of faces relation

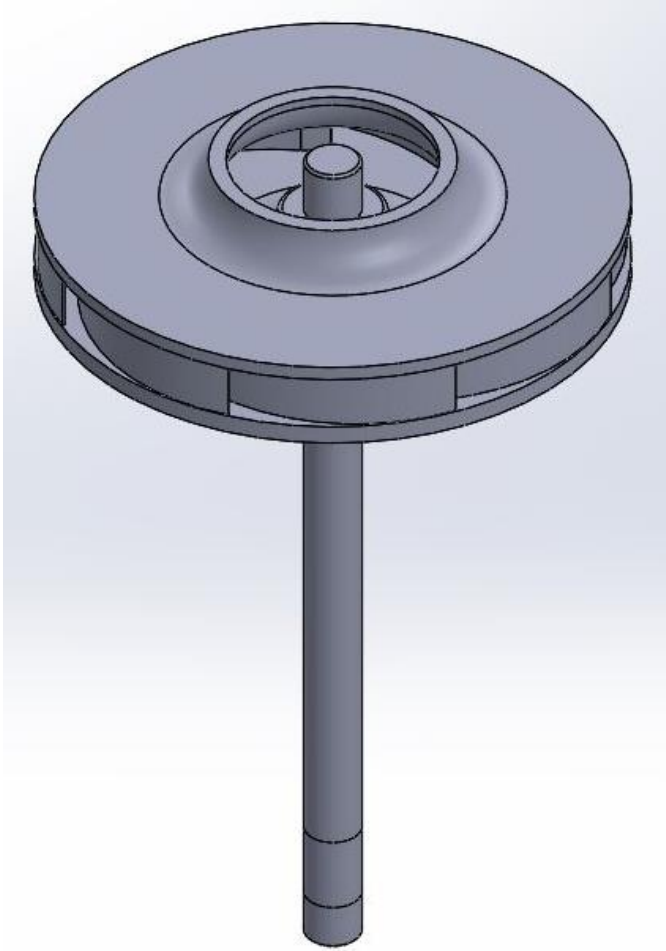


Figure 3.31: AS1 (assembly with shaft 1)

Now we are going to explain how the other shafts were made, although all they started from the same base as the IBS2 shaft. As we have seen in Figure 3.26, the first step was to create a sketch with a circumference of 5,92 mm in diameter, but the extrusion followed the equation (3.2).

$$\text{Shaft height} = 95 - 6 - (10 - \text{hole depth}) \quad (3.2)$$

Originally the shaft was 95 mm long, as we wanted that the distance between the base of the impeller and the end where the axis began to rotate was the same for all cases, the 6 mm protruding from the through hole were subtracted, and, the difference between the whole hole and the actual depth of the hole. Therefore, in the case of IBS2, the shaft was 88,7 mm long.

The shaft had to fit in the notch that was made to the hole in the impeller, therefore we used the revolve cut tool before making a sketch like the one in Figure 3.22, in the side view plane, as seen in Figure 3.32. The result is shown in Figure 3.33.

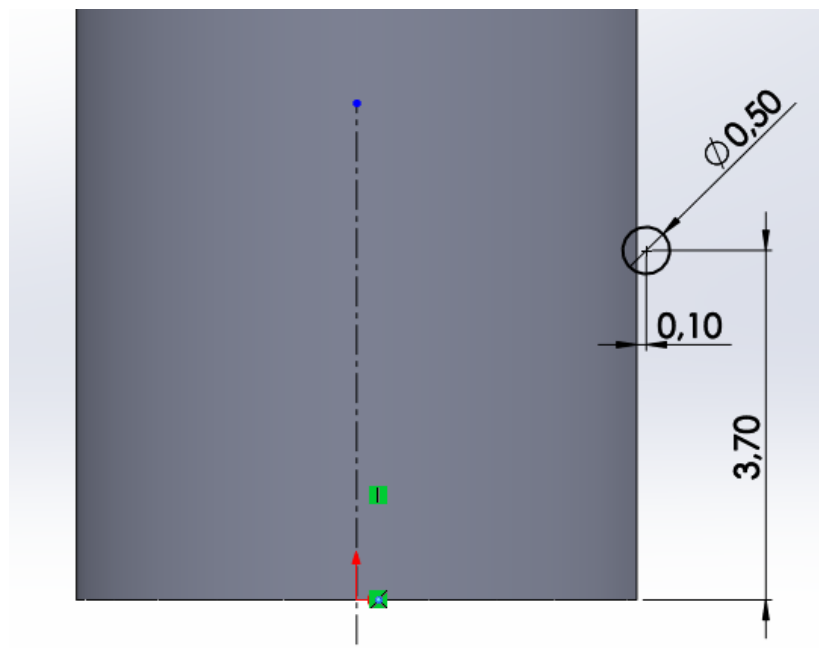


Figure 3.32: Revolve cut sketch for S2

As we can see, the measurements correspond to the same ones that we could do in the hole of the impeller (Figure 3.22).

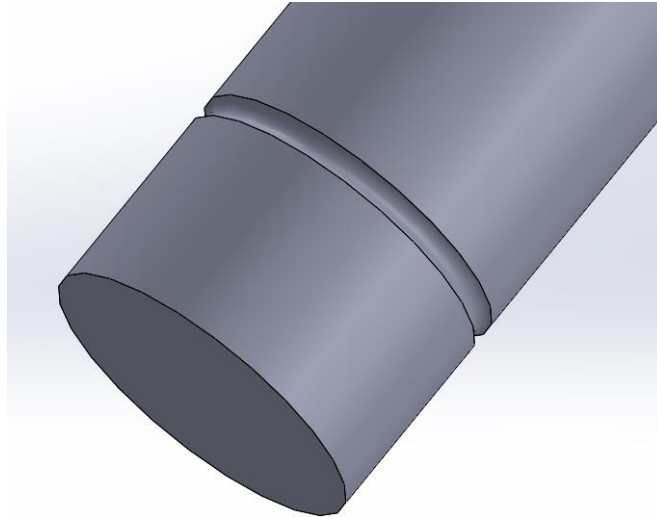


Figure 3.33: Shaft for IBS2. Step 2

The next step was to machine the flat face, so using the same measurements at the base of the shaft as in Figure 3.24, a cut of 14 mm in length was made, as in Figure 3.34.

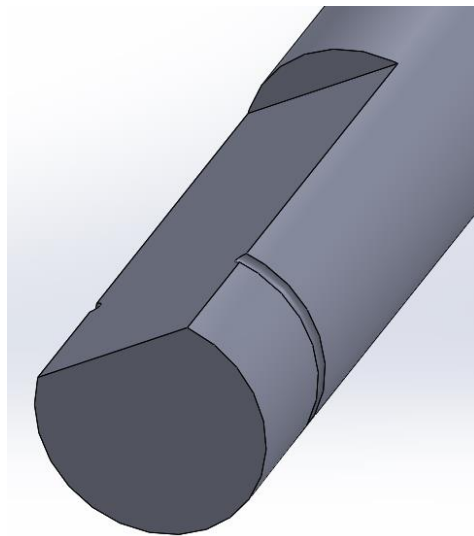


Figure 3.34: Shaft for IBS2. Step 3

Then, the aesthetic part was made to the shaft, which consisted of making a chamfer at both ends with the same measures as with the axis of IBS1, and a rounding of 1 mm at the vertex of separation between the flat face and the cylindrical face (Figure 3.35).

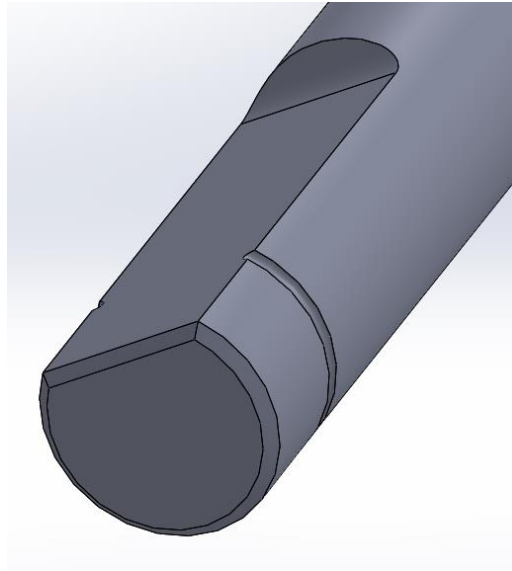


Figure 3.35: Shaft for IBS2. Step 4

The last step, in Figure 3.36, was to create the three split lines again. The only one that had different measurements was that in IBS1 was placed 16 mm from the end, in this case we placed the lower line at the same distance as the hole had in depth, in case of IBS2, 9,7 mm.

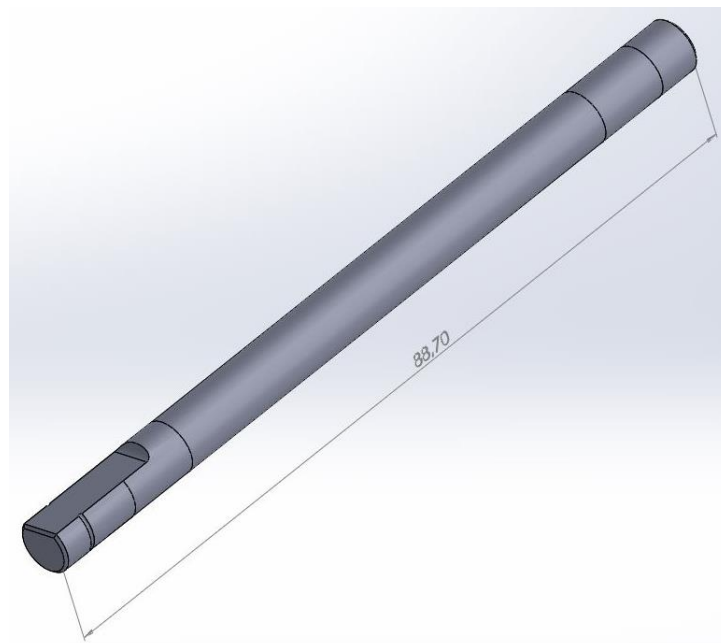


Figure 3.36: Shaft for IBS2. Step 5

For the assembly of IBS2 and the subsequent 3 pieces were used as well, which were IC1, IBS2 and S2. As previously mentioned, the relationships between IC1 and IBS2 were clear and there is still a need to explain how to assemble S2. First, a concentricity relation was used with the hole of the impeller, then a coincidence of faces was used between the flat

faces of S2 and IBS2 and finally we made the face of the base of the impeller hole coincide with the face of the base from the shaft. The final result is in Figure 3.37, and also we can see the overall view of the internal design in Figure 3.38.

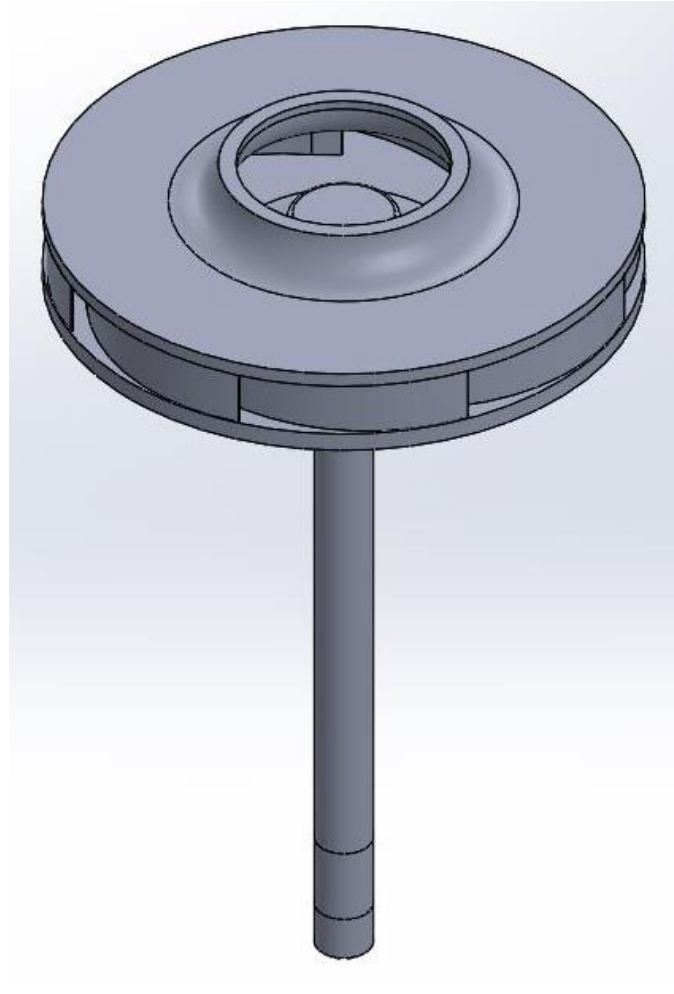


Figure 3.37: AS2 (assembly with shaft 2)

As was done in Table 3.9, we have done the same in Table 3.11 for the internal design.

Table 3.11: Overall view of the formation of assemblies for internal design

| | | | | | | |
|------|---|-----|---|----|---|-----|
| IBS1 | + | IC1 | + | S1 | = | AS1 |
| IBS2 | + | IC1 | + | S2 | = | AS2 |
| IBS3 | + | IC1 | + | S3 | = | AS3 |
| IBS4 | + | IC1 | + | S4 | = | AS4 |
| IBS5 | + | IC1 | + | S5 | = | AS5 |
| IBS6 | + | IC1 | + | S6 | = | AS6 |

| | | | | | | |
|-------|---|-----|---|-----|---|------|
| IBS7 | + | IC1 | + | S7 | = | AS7 |
| IBS8 | + | IC1 | + | S8 | = | AS8 |
| IBS9 | + | IC1 | + | S9 | = | AS9 |
| IBS10 | + | IC1 | + | S10 | = | AS10 |

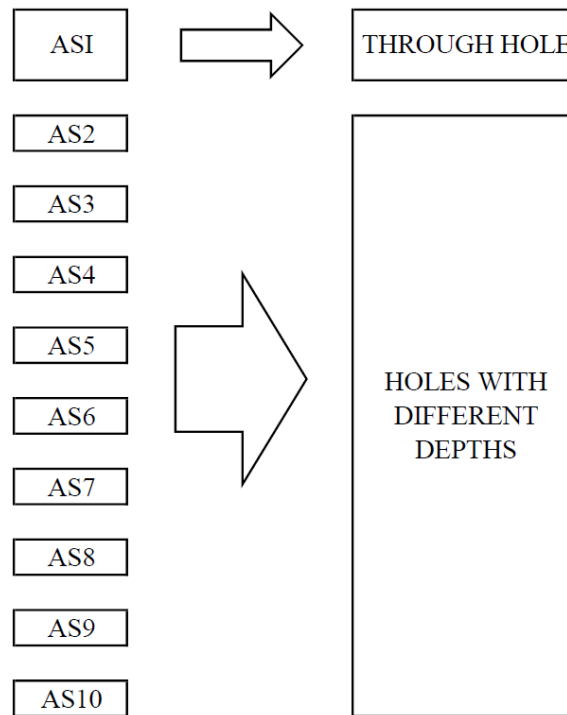


Figure 3.38: Overall view of internal design

3.2. Practical section

In this section, we are going to describe the used methodology to study the selection of the final material and for the final external and internal design. For this, Ansys software has been used, specialized in simulations of product behaviour in different situations, and more specifically its module called Workbench, with a better working interface. So, starting from section 3.1 and the aforementioned, we are going to explain the practical part.

3.2.1. Simulations to select the material

To select the final material of which the impeller is composed, three different types of simulation were carried out. And when we say different, we mean that the first one has been made with the approximate impeller A1 explained in section 3.1.2.1, and at room temperature of 22 °C. The second was an approximation to the properties that would have

the same materials at 120 °C, point of maximum working temperature imposed with the same approximate impeller A1, and finally, the same approach to the temperature of 120 °C with the impeller model provided by the company.

The first step was to select what type of test we wanted to do once the Ansys Workbench module was started and place it on the Project Schematic to start working on it. In this section, all the simulations were carried out through the Static Structural analysis system, as we can see in Figure 3.39.

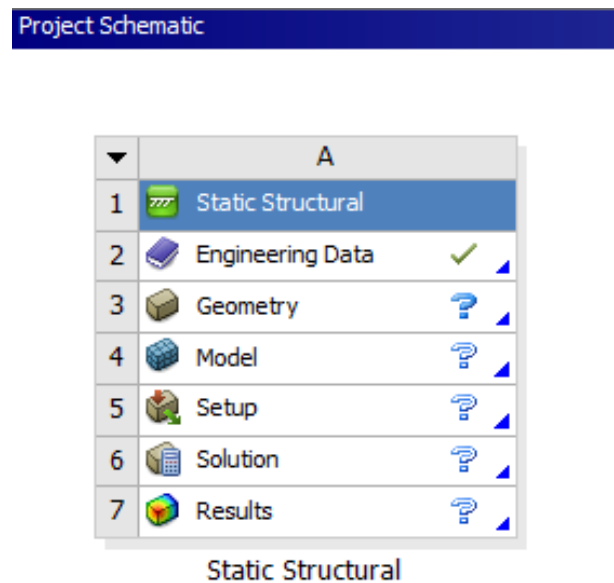


Figure 3.39: Project schematic in the starting point [16]

The next step was to review the Engineering Data. By default, we had Structural Steel as material to assign to the object and perform the simulation, and Workbench also had a database of generic materials to change this by default. However, we wanted some materials that were not defined, and we had to create them with the properties of Table 3.12. These properties were at room temperature, since later we will talk about the simulations with the same materials at different temperatures, so that some properties changed. For the same assembly, the weights according to the material selected were the following, seen in Table 3.13.

Table 3.12: Assigned properties to each material at 22 °C [6]

| Material | PA66 (30% glass fiber, lubricated) | PA66 (40% long glass fiber) | PA66 (50% long glass fiber) | PA66 (40% glass fiber, lubricated) | PA6 (50% long glass fiber) | PA66 (50% glass fiber) | PA66 (40% long glass fiber, lubricated) | PA66 (50% long glass fiber, lubricated) |
|-------------------------------------------|---------------------------------------------|-----------------------------------------|-----------------------------------------|---------------------------------------------|----------------------------------------|---------------------------------|--------------------------------------------------|--------------------------------------------------|
| Density [kg/m ³] | 1445 | 1460 | 1565 | 1535 | 1555 | 1575 | 1570 | 1620 |
| Young's Modulus [GPa] | 8,91 | 10 | 11,8 | 11,85 | 12,2 | 12,25 | 13,85 | 15,25 |
| Poisson's Ratio | 0,35 | 0,35 | 0,34 | 0,35 | 0,35 | 0,34 | 0,35 | 0,34 |
| Bulk Modulus [GPa] | 9,89 | 10,89 | 12,03 | 12,91 | 13,56 | 12,45 | 15,09 | 15,55 |
| Shear Modulus [GPa] | 3,3 | 3,71 | 4,41 | 4,4 | 4,52 | 4,58 | 5,14 | 5,71 |
| Tensile Yield Strength [MPa] | 152,5 | 160 | 175 | 150,5 | 170 | 175 | 220,5 | 203,5 |
| Compressive Yield Strength [MPa] | 129,5 | 192 | 210,5 | 131 | 204 | 211,5 | 278 | 304 |
| Tensile Ultimate Strength [MPa] | 159 | 160 | 175,5 | 186 | 170 | 176,5 | 231 | 253,5 |

Table 3.13: Corresponding weight to each material [6]

| Material | PA66 (30% glass fiber, lubricated) | PA66 (40% long glass fiber) | PA66 (50% long glass fiber) | PA66 (40% glass fiber, lubricated) | PA6 (50% long glass fiber) | PA66 (50% glass fiber) | PA66 (40% long glass fiber, lubricated) | PA66 (50% long glass fiber, lubricated) |
|----------|------------------------------------------------|-----------------------------------------|-----------------------------------------|------------------------------------------------|----------------------------------------|---------------------------------|-----------------------------------------------------|-----------------------------------------------------|
| Mass [g] | 20,45 | 20,66 | 22,15 | 21,73 | 22,01 | 22,29 | 22,22 | 22,93 |

Once the materials were created, the next step was to import the geometry into the Design Modeler module, usually in step or xt format (Parasolid) so that there are no compatibility errors. To do this we went to File - Import External Geometry File, and once opened, we clicked on Generate. This done, everything was ready to go to the Mechanical module with which we traced the mesh, we fixed supports for the impeller, we applied external forces and we saw what results we got.

In the Mechanical module, we assigned the same material to both parts (IB1 and IC1) within the Geometry - Piece - Material - Assignment tab. We changed the coordinate system to cylindrical, as shown in Figure 3.40, instead of cartesian in which the main axes were Z and X. The connections between both parts were made automatically, although it was necessary to change the mesh to obtain greater precision in the subsequent results. For this we went to Mesh - Defaults and in Element Order we chose Quadratic instead of being controlled by the program as it came by default. In addition, the mesh size was assigned to 1 mm.

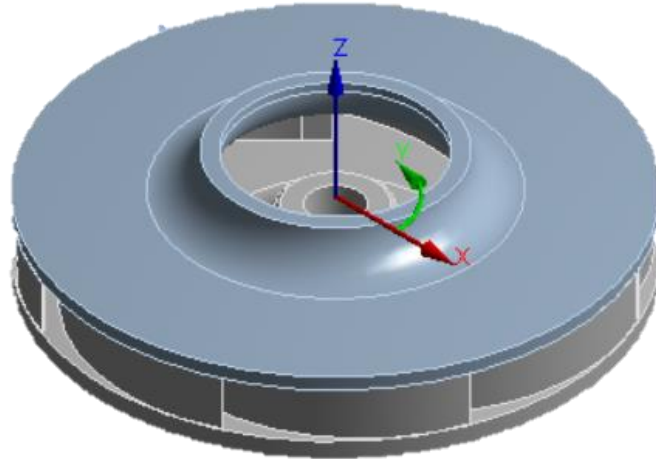


Figure 3.40: Cylindrical Coordinate System

So that there was not a great computational time, the simulation time was defined in 20 seconds, with a constant rotation speed of 60000 rpm and a cylindrical support in the shaft gap, where we fixed the radial and axial movement, and left as free for the rotation, the tangential movement. The results that we obtained corresponded to the total deformation, to the deformation in radial direction and to the equivalent stress of von-Mises.

Finally, we had to carry out this procedure for each of the materials mentioned in Table 3.12. In addition, not only do we kept the results obtained from this analysis, but we also conducted a study with the same impeller at the temperature of 120 °C, with the properties of Table 3.14, and another study at 120 °C with the impeller of the company.

Table 3.14: Assigned properties to each material at 120 °C

| Material | PA6 (50% long glass fiber) | PA66 (30% glass fiber, lubricated) | PA66 (40% glass fiber, lubricated) | PA66 (40% long glass fiber) | PA66 (40% long glass fiber, lubricated) | PA66 (50% glass fiber) | PA66 (50% long glass fiber) | PA66 (50% long glass fiber, lubricated) |
|-----------------------|----------------------------------------|------------------------------------------------|------------------------------------------------|-----------------------------------------|-----------------------------------------------------|---------------------------------|-----------------------------------------|-----------------------------------------------------|
| Young's Modulus [GPa] | 7,13 | 3,31 | 2,55 | 2,15 | 2,98 | 5,69 | 5,48 | 7,08 |
| Bulk Modulus [GPa] | 7,92 | 3,68 | 2,78 | 2,35 | 3,25 | 5,78 | 5,58 | 7,22 |
| Shear Modulus [GPa] | 2,64 | 1,23 | 0,95 | 0,8 | 1,11 | 2,13 | 2,05 | 2,65 |

It was not easy to obtain the parameters of Table 3.14 since they are specific tests that the material manufacturers carry out in their products, however, through an online catalogue of the manufacturer DuPont Corporation, we were able to reach an approximation of them.

Taking as an example PA6 (50% glass fiber), the graph of Figure 3.41 was obtained. The material was called DuPont Zytel 73G50HSLA BK416 and it was the one that most resembled the material we wanted.

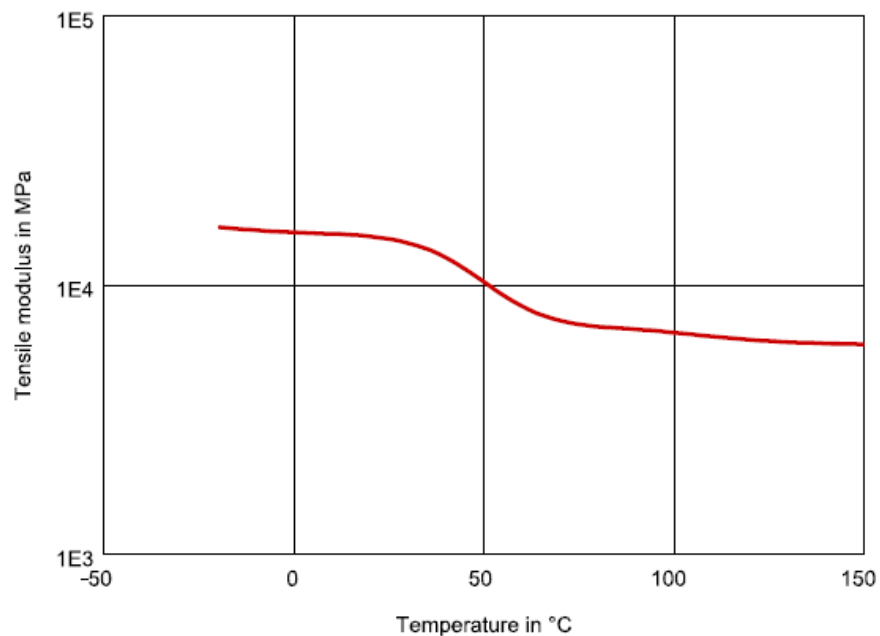


Figure 3.41: PA6 (50% glass fiber). Tensile modulus (MPa) vs. Temperature (°C) [17]

Obtaining from the graph the tensile modulus for 22 °C, we observed that it was not the same as we had in the datasheet provided by the CES EduPack 2017 software, so we had to iterate to obtain the value of the approximate tensile modulus for 120 °C.

Therefore, knowing that our value for the tensile modulus (or shear modulus) was 4520 MPa, and that in the graph it was 15850 MPa at 22 °C, we calculated that it would be equal to 2640 MPa since in the graph it was 9260 MPa.

By means of the equation (3.3), substituting the value of the shear modulus and the Poisson's ratio, we obtained the Young's modulus.

$$E = 2 \cdot G(1 + \nu) \tag{3.3}$$

And the same procedure with the equation (3.4), to calculate the bulk modulus.

$$K = \frac{E}{3(1 + \nu)} \tag{3.4}$$

Once this is done, we calculated all the properties mentioned for all the materials, using the same procedure above. Furthermore, once the three tests with all the materials were done, we obtained the results that will be shown in section 4.1. We can see the overall view of material simulations in Figure 3.42.

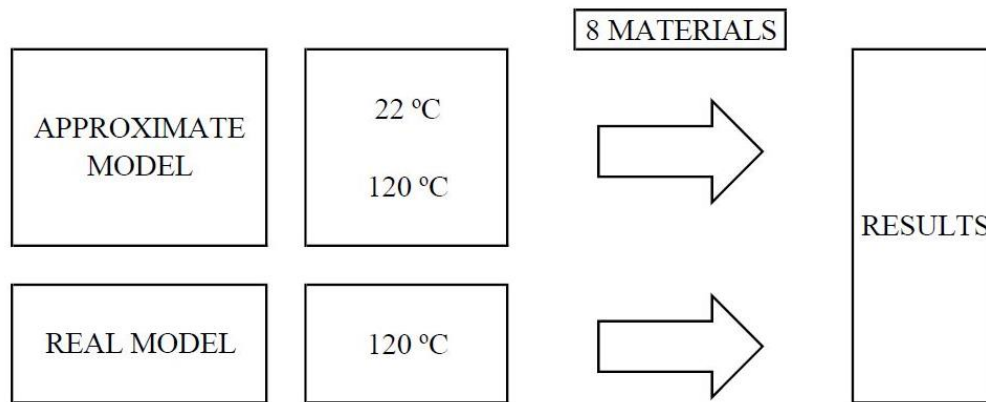


Figure 3.42: Overall view of material simulations

3.2.2. Simulations to select the external design

In these simulations to select the best external design, we used the same analysis as in section 3.2.1, Static Structural. We started with A1, and once the study was finished, we proceeded to do the same with the other nine assemblies.

For the external design to influence the tensions and deformations, all the assemblies had the same material, PA6 (50% long glass fiber). In addition, the properties were the same as in Table 3.14, that is, as if we were testing at 120°.

Then, we imported A1 as explained in section 3.2.1, the mesh was created in the same way and the supports and external loads were fixed as in Figure 3.43.

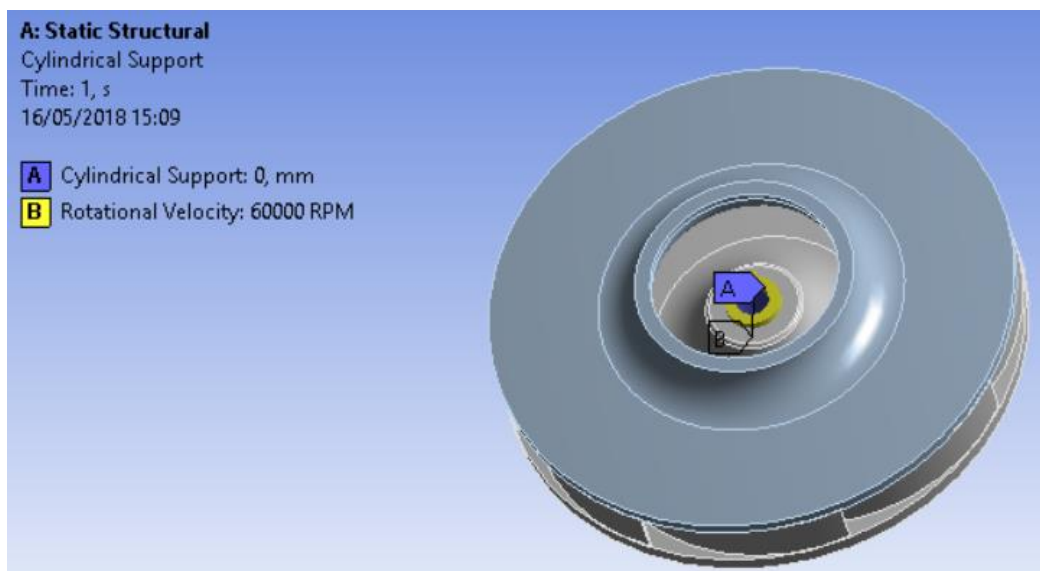


Figure 3.43: Environment conditions for external design simulations

The last step was to select the solution type that we wanted to obtain, and it as was done in section 3.2.1, we selected the total deformation, the deformation in radial direction and the equivalent stresses. We can see the project tree for the external design in Figure 3.44 and the overall view of the external design simulations in Figure 3.45.

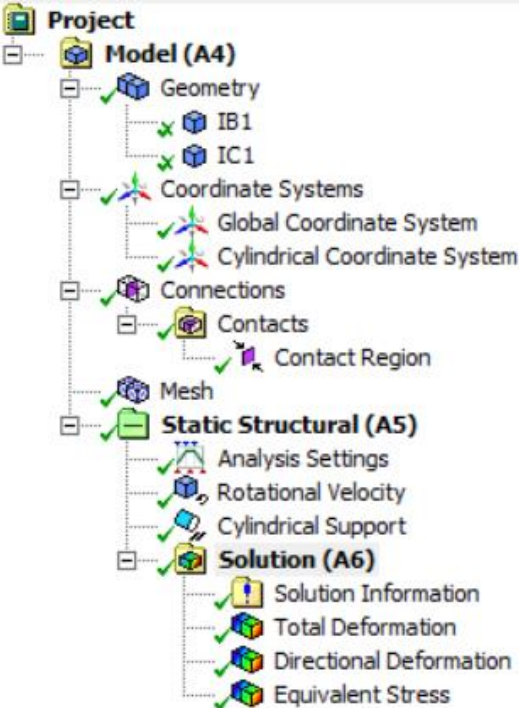


Figure 3.44: Project tree for the external design [16]

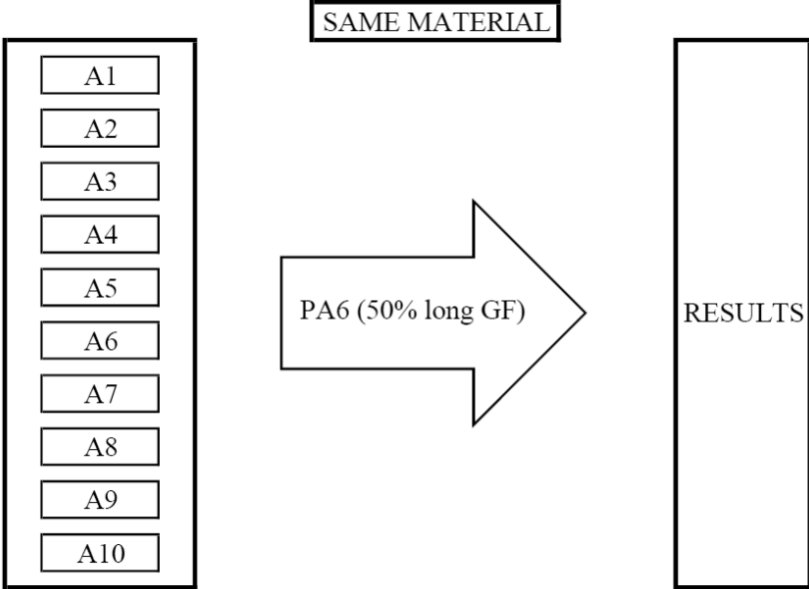


Figure 3.45: Overall view of external design simulations

3.2.3. Simulations to select the internal design

The simulations to select the best internal design were different to the simulations done to select the ideal material and the external design. In this case, instead of being a Static Structural analysis, it was a Modal analysis, or what is the same, a vibration analysis. This type of analysis was chosen because it was important to know if the proposed solution in section 2.5.4, different from the others discussed in section 2.5, would be better.

In this case, we worked with the models designed in section 3.1.2.2, therefore, in addition to having the impeller present in the simulation, the shaft was also present.

The first steps were like those of the previous two sections. The Engineering Data was the same as in Table 3.14, that is, with the properties of the materials at 120°. As for the Geometry, the assemblies were imported to each study that was made, from AS1 to AS10.

Once inside the Mechanical module, all the assemblies were imposed on the same materials, so that the only variation in the solutions was due to the internal design. The shaft was made of Structural Steel, and the two pieces of the impeller were made of PA6 (50% long glass fiber). In addition, a cylindrical coordinate system was created again to evaluate better the results. The mesh, however, was made with the same parameters as the previous sections.

It was imposed a maximum of 9 modes inside Modal to find within Analysis Settings, a rotation speed of 60000 rpm, and two cylindrical supports, corresponding to the bearings, and located in the positions where the split lines were created in section 3.1.2.2. This type of supports, shown in Figure 3.46, were placed on the shaft simulating the bearings since we were not interested in the shaft, but yes in the connection of this with the impeller and the same impeller.

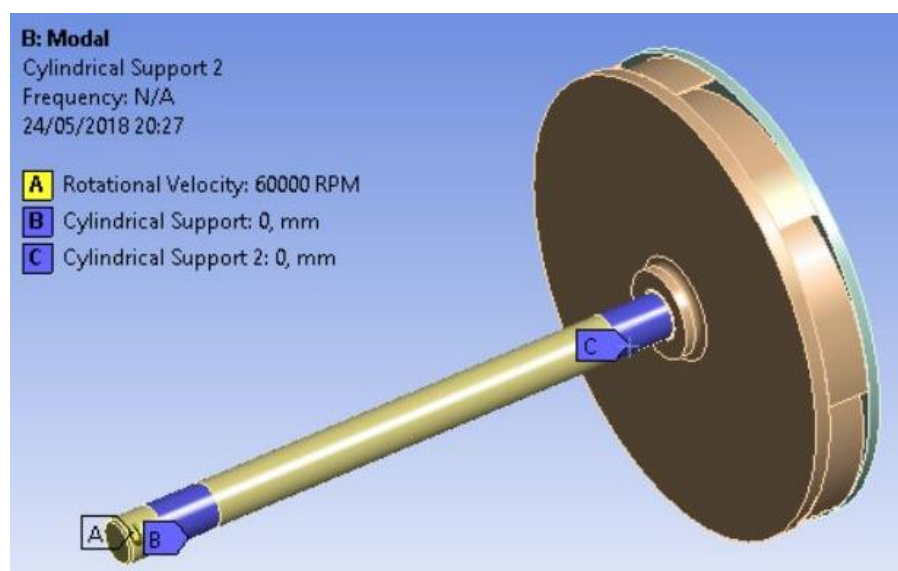


Figure 3.46: Environment conditions for internal design simulations

The solution was evaluated by total deformation. But despite of this, the frequencies in which system were, were the most important values since being near one of them meant that the system was vibrating a lot, whereby would be a bad design. We can see the overall view of the internal design simulations in Figure 3.47.

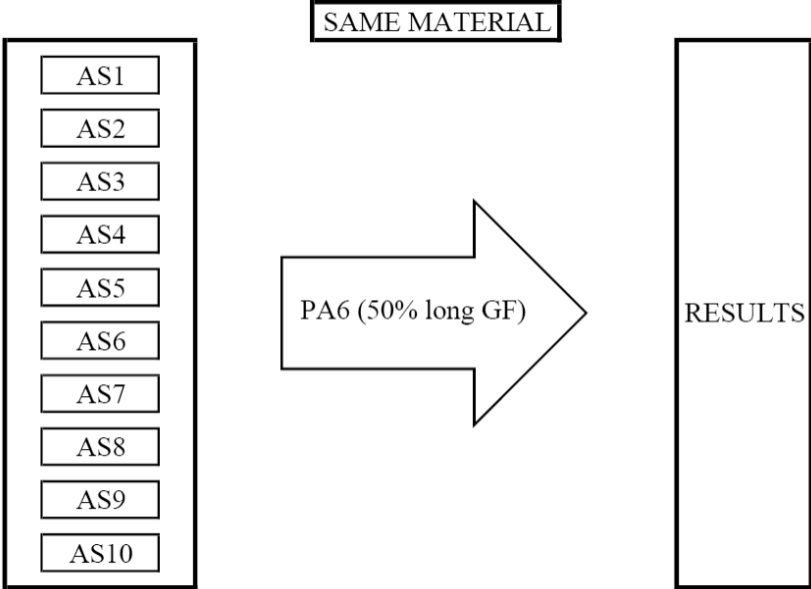


Figure 3.47: Overall view of internal design simulations

4. Results

In this section the results of the simulations carried out in section 3.2 will be exposed and briefly commented, and we will leave for the next section, the discussion of these more deeply.

4.1. Material selection

Next, we are going to present the results corresponding to the simulations carried out to select the best material. Each table corresponds to a test that was made with different properties. In Table 4.1, we have the test carried out at room temperature, in Table 4.2 we have the test carried out at 120 °C, and finally, in Table 4.3 we have the test carried out at 120 °C with the model of the impeller provided by the company. Also in Figure 4.1 and in Figure 4.2, we are able to see the minimum and maximum points for the approximate model and for the real model.

Table 4.1: Results for material simulations at 22 °C [16]

| Material | Total Deformation [mm] | | Deformation in radial direction [mm] | | Equivalent (von-Misses) Stress [MPa] | |
|-----------------------------------------|------------------------|---------|--------------------------------------|---------|--------------------------------------|---------|
| | Minimum | Maximum | Minimum | Maximum | Minimum | Maximum |
| PA66 (50% long glass fiber, lubricated) | 0,068 | 0,684 | -0,007 | 0,052 | 0,165 | 106,57 |
| PA66 (40% long glass fiber, lubricated) | 0,071 | 0,721 | -0,007 | 0,056 | 0,169 | 102,31 |
| PA6 (50% long glass fiber) | 0,077 | 0,781 | -0,008 | 0,063 | 0,169 | 101,06 |

Results

| | | | | | | |
|------------------------------------|-------|-------|--------|-------|-------|--------|
| PA66 (50% glass fiber) | 0,092 | 0,931 | -0,008 | 0,063 | 0,16 | 103,67 |
| PA66 (40% glass fiber, lubricated) | 0,085 | 0,854 | -0,008 | 0,064 | 0,165 | 100,03 |
| PA66 (50% long glass fiber) | 0,092 | 0,925 | -0,008 | 0,065 | 0,16 | 102,97 |
| PA66 (40% long glass fiber) | 0,083 | 0,842 | -0,009 | 0,072 | 0,157 | 95,145 |
| PA66 (30% glass fiber, lubricated) | 0,112 | 1,127 | -0,01 | 0,08 | 0,157 | 93,931 |

Table 4.2: Results for material simulations at 120 °C [16]

| Material | Total Deformation [mm] | | Deformation in radial direction [mm] | | Equivalent (von-Mises) Stress [MPa] | |
|-----------------------------------------|------------------------|---------|--------------------------------------|---------|-------------------------------------|---------|
| | Minimum | Maximum | Minimum | Maximum | Minimum | Maximum |
| PA66 (50% long glass fiber, lubricated) | 0,16 | 1,618 | -0,015 | 0,113 | 0,165 | 106,64 |
| PA66 (40% long glass fiber, lubricated) | 0,347 | 3,5 | -0,034 | 0,258 | 0,169 | 102,51 |
| PA6 (50% long glass fiber) | 0,141 | 1,427 | -0,014 | 0,107 | 0,169 | 101,1 |
| PA66 (50% glass fiber) | 0,197 | 1,993 | -0,018 | 0,137 | 0,16 | 103,75 |
| PA66 (40% glass fiber, lubricated) | 0,389 | 3,923 | -0,039 | 0,295 | 0,165 | 100,26 |
| PA66 (50% long glass fiber) | 0,207 | 2,089 | -0,018 | 0,141 | 0,16 | 103,05 |
| PA66 (40% long glass fiber) | 0,457 | 4,619 | -0,044 | 0,333 | 0,157 | 95,407 |
| PA66 (30% glass fiber, lubricated) | 0,266 | 2,686 | -0,028 | 0,214 | 0,157 | 94,036 |

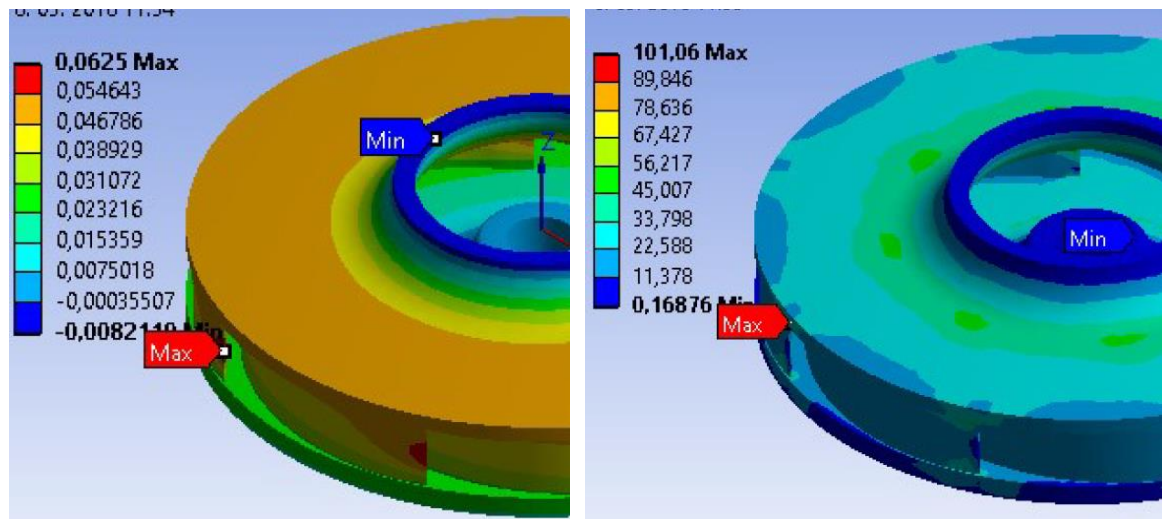


Figure 4.1: Minimum and maximum points in the approximate model [16]

Table 4.3: Results for material simulations at 120 °C with the real impeller [16]

| Material | Total Deformation [mm] | | Deformation in radial direction [mm] | | Equivalent (von-Mises) Stress [MPa] | |
|-----------------------------------------|------------------------|---------|--------------------------------------|---------|-------------------------------------|---------|
| | Minimum | Maximum | Minimum | Maximum | Minimum | Maximum |
| PA66 (50% long glass fiber, lubricated) | 0,079 | 0,789 | 0 | 0,096 | 0,197 | 204,57 |
| PA66 (40% long glass fiber, lubricated) | 0,181 | 1,8 | 0 | 0,221 | 0,176 | 195,77 |
| PA6 (50% long glass fiber) | 0,075 | 0,746 | 0 | 0,092 | 0,17 | 194,1 |
| PA66 (50% glass fiber) | 0,096 | 0,955 | 0 | 0,116 | 0,192 | 198,64 |
| PA66 (40% glass fiber, lubricated) | 0,206 | 2,062 | 0 | 0,253 | 0,172 | 191,23 |
| PA66 (50% long glass fiber) | 0,099 | 0,985 | 0 | 0,12 | 0,19 | 197,5 |
| PA66 (40% long glass fiber) | 0,233 | 2,324 | 0 | 0,285 | 0,164 | 181,73 |
| PA66 (30% glass fiber, lubricated) | 0,149 | 1,492 | 0 | 0,184 | 0,158 | 179,9 |

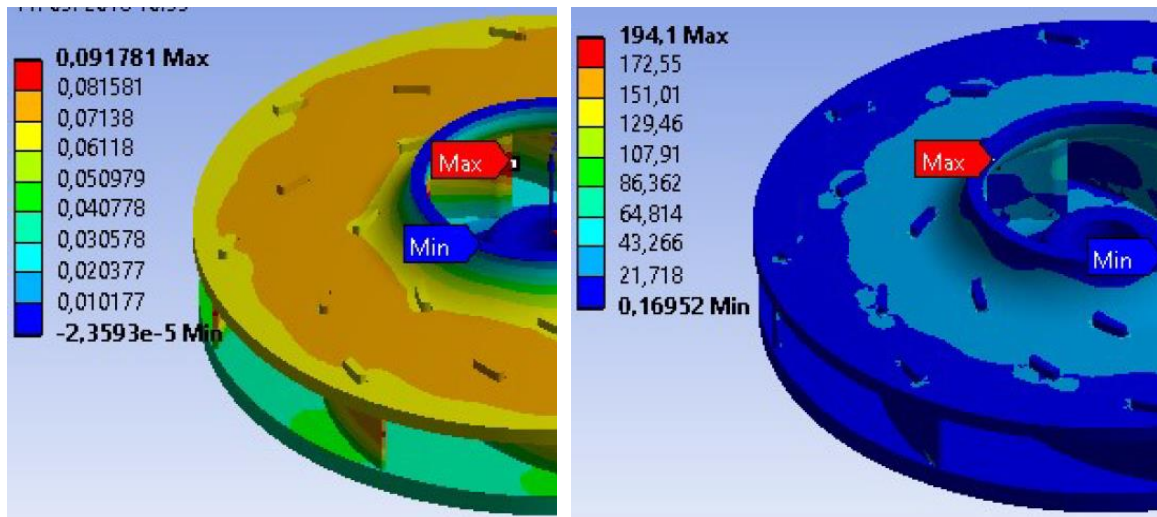


Figure 4.2: Minimum and maximum points in the real model [16]

As we can see, the Table 4.1 is ordered from lowest to highest value of maximum deformation on the X axis. The other two tables have maintained the same order for the materials.

We want to consider that not following the order of least maximum deformation in the X axis, it will turn out to be better material than another. All the resulting values have been taken into account, and the final selection will be explained in the next section regarding the discussion of results.

4.2. Design of the impeller

Next, we are going to separate the results of the simulations for the external design and for the internal design.

Although there has not been a simulation to verify that the product will resist a minimum of 15000 start/stop cycles, because it does not exist either, this characteristic was dependent on having chosen a suitable material, having an optimal design and that the connections are the corresponding ones .

4.2.1. External design

In the following table, the results of each test applied to each assembly are shown, analysing as in the previous section, the total deformation, the deformation in radial direction and the resulting equivalent stresses.

Table 4.4: Results for external design simulations [16]

| Assembly | Total Deformation [mm] | | Deformation in radial direction [mm] | | Equivalent (von-Mises) Stress [MPa] | |
|----------|------------------------|---------|--------------------------------------|---------|-------------------------------------|---------|
| | Minimum | Maximum | Minimum | Maximum | Minimum | Maximum |
| A1 | 0,139 | 1,405 | -0,014 | 0,107 | 0,169 | 101,1 |
| A2 | 0,016 | 4,345 | -0,019 | 0,109 | 0,074 | 97,515 |
| A3 | 0,013 | 3,727 | -0,017 | 0,108 | 0,149 | 95,376 |
| A4 | 0,084 | 23,52 | -0,02 | 0,111 | 0,073 | 112,61 |
| A5 | 0,026 | 7,323 | -0,021 | 0,011 | 0,115 | 114,73 |
| A6 | 0,035 | 9,619 | -0,024 | 0,114 | 0,083 | 116,73 |
| A7 | 1,415 | 394 | -0,024 | 0,114 | 0,048 | 136,15 |
| A8 | 0,001 | 66,908 | -0,024 | 0,113 | 0,039 | 108,8 |
| A9 | 0,015 | 4,109 | -0,017 | 0,109 | 0,052 | 104,8 |
| A10 | 0,02 | 5,651 | -0,017 | 0,108 | 0,154 | 101,59 |

This time, and as already explained in previous sections, the material applied to all the assemblies was the same (PA6 50% long glass fiber) so that the results varied only due to the change of external dimensions.

To verify that the selection of the external design is appropriate, we can check the generated torque at the start moment in the following table.

Table 4.5: Generated torques

| Assembly | Torque τ [N·m] |
|----------|---------------------|
| A1 | 0,089 |
| A2 | 0,075 |
| A3 | 0,082 |
| A4 | 0,083 |
| A5 | 0,082 |
| A6 | 0,077 |
| A7 | 0,080 |
| A8 | 0,082 |
| A9 | 0,075 |
| A10 | 0,082 |

The final selection, as discussed in section 4.1, will be explained in section 5.

4.2.2. Internal design

The frequency of our impeller was 1000 Hz since it is the rotation speed divided by the number of seconds in a minute. Therefore, depending on the frequency of each mode, if our frequency value was close to one of these, it was detrimental to the system.

At each test, we saw a graph like the one in Figure 4.3. In it we can see the frequency of each mode.

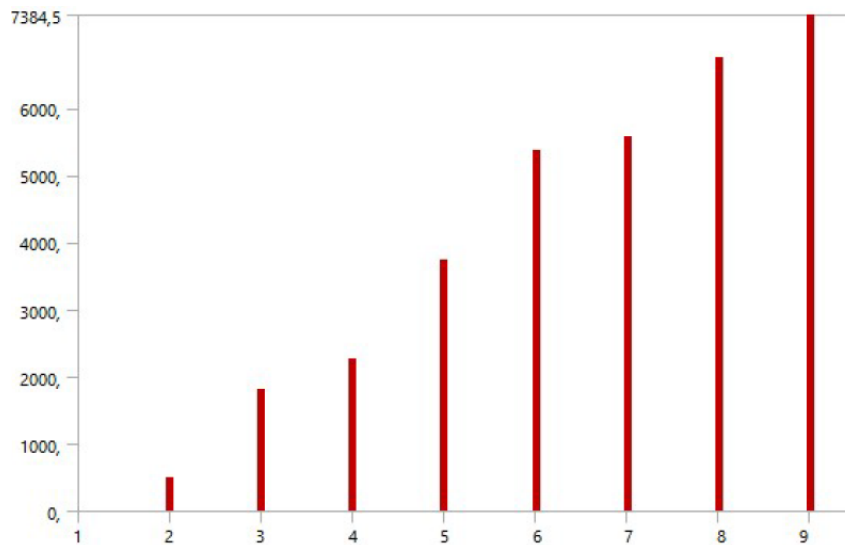


Figure 4.3: Vibration modes in AS1 [16]

In all assemblies, the impeller was maintained between modes 2 and 3, so we can see the results in Table 4.6.

Table 4.6: Frequencies in modes 2 and 3 [16]

| Assembly | Damped Frequency in Mode 2 [Hz] | Damped Frequency in Mode 3 [Hz] |
|----------|---------------------------------|---------------------------------|
| AS1 | 499,43 | 1801,30 |
| AS2 | 486,65 | 1797,10 |
| AS3 | 485,49 | 1795,20 |
| AS4 | 486,39 | 1796,60 |
| AS5 | 482,01 | 1792,20 |
| AS6 | 481,67 | 1792,20 |
| AS7 | 485,07 | 1794,80 |
| AS8 | 484,19 | 1793,90 |
| AS9 | 486,28 | 1796,50 |
| AS10 | 483,50 | 1793,20 |

Furthermore, in Figure 4.4 and Figure 4.5, we can see what the vibration is like in each mode.

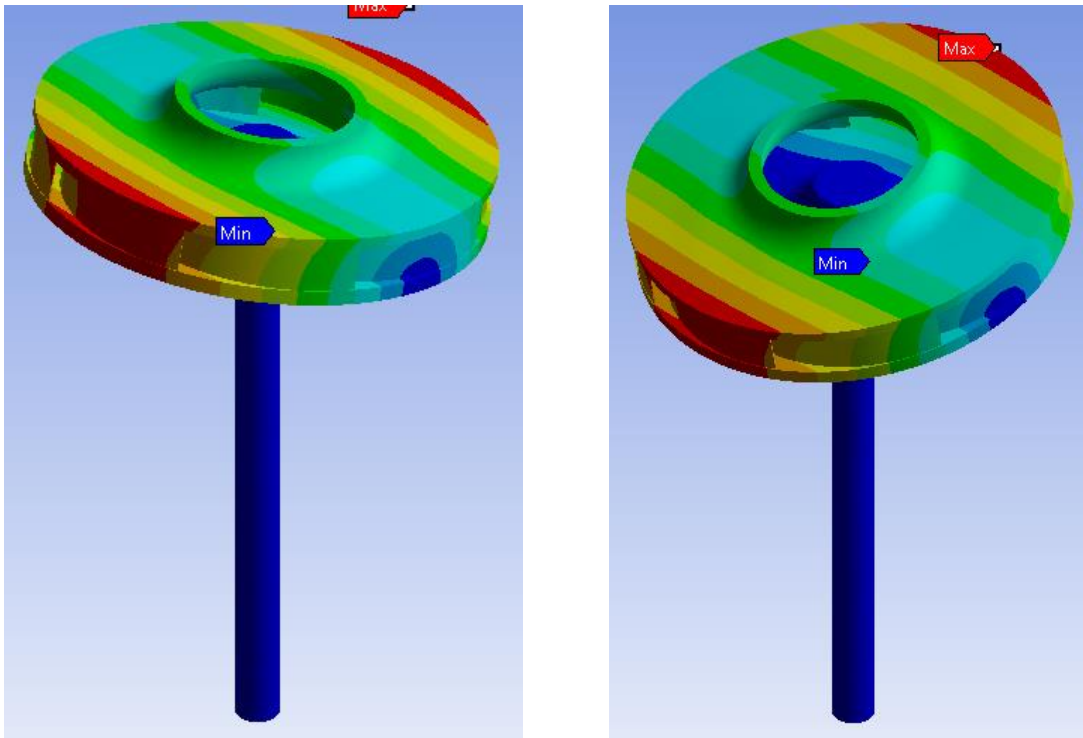


Figure 4.4: Vibration movement in Mode 2 [16]

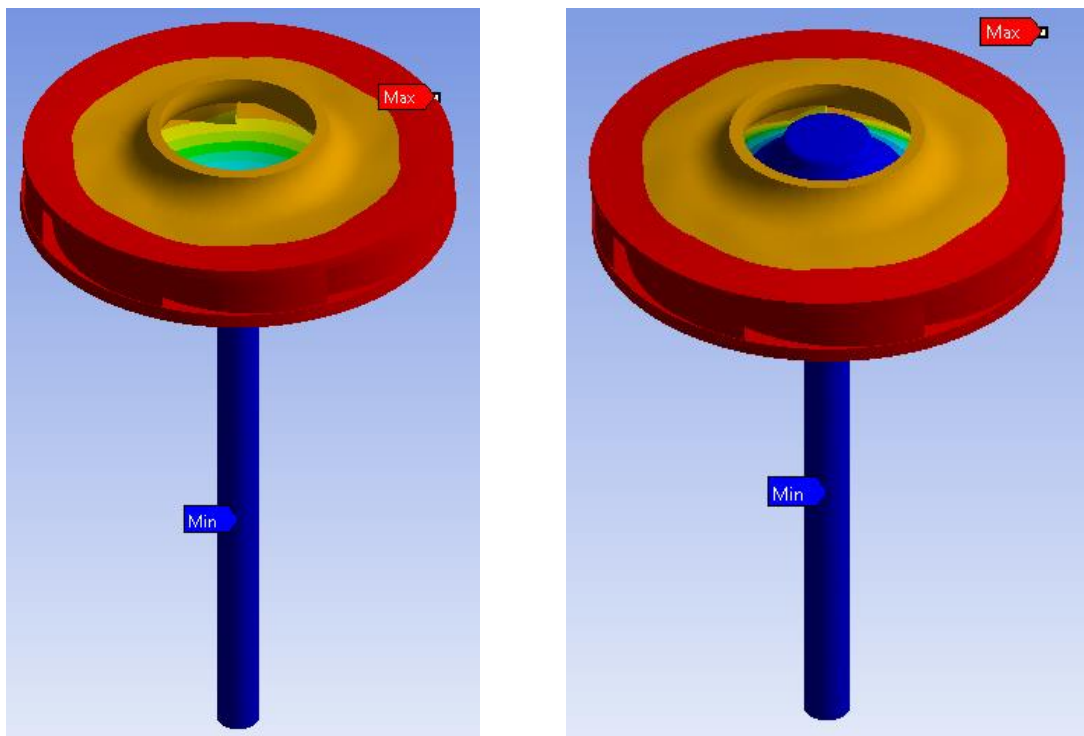


Figure 4.5: Vibration movement in Mode 3 [16]

As explained in the other results sections, these will be discussed in section 5

5. Discussion

In this section we will decide how our impeller will finally be, after obtaining the results of the simulations and having theoretical knowledge for the joining technologies. First, the material to be used will be defined, and then we will know the joining method of the two pieces of the impeller. Afterwards, we will talk about the design, finishing with the union method between the impeller and the shaft.

5.1. Material

After obtaining the values in Table 4.1, Table 4.2, and Table 4.3, the results were normalized to know which material behaved better in terms of stresses and deformations.

For this, starting with the results of the Table 4.1, and operating in the same way in the two remaining tables, all the values of each column were added and then each value of each cell was divided by that sum, in such a way that it gave us the percentages of each material.

Since not all the columns provided a value like the real one as is the case of the maximum stress, because it was located at a point of union between the blade and the cover, and around the tensions were much lower as we can see in the Figure 4.1, the previous percentages were normalized multiplying by certain coefficients. It is necessary to comment that this decision was subjective, since each data was valued according to our criterion.

The two columns of total deformation were multiplied by 0,375, by 0,5 the two columns of deformation in radial direction and the one of minimum stresses located in a point, and by 0,125 the column of maximum stresses located in a point.

As mentioned previously, this was done for all three cases. For all materials at 22 °C, for all materials at 120 °C and for all materials at 120 °C with the real model.

Afterwards, the price per kilo of each material (Table 5.1) was also assessed, and it was normalized by multiplying the value by 0,5.

Table 5.1: Material prices [6]

| Material | Price [€/kg] |
|-----------------------------------------|--------------|
| PA66 (50% long glass fiber, lubricated) | 4,14 |
| PA66 (40% long glass fiber, lubricated) | 4,35 |
| PA6 (50% long glass fiber) | 2,86 |
| PA66 (50% glass fiber) | 2,47 |
| PA66 (40% glass fiber, lubricated) | 3,68 |
| PA66 (50% long glass fiber) | 3,13 |
| PA66 (40% long glass fiber) | 3,34 |
| PA66 (30% glass fiber, lubricated) | 3,88 |

Finally, we add each percentage and the one that had a lower value, was the one indicated to be used.

Table 5.2: Example of standardization for materials

| Material | Total Deformation [mm] | | Deformation in radial direction [mm] | | Equivalent (von-Misses) Stress [MPa] | | Price [€/kg] |
|------------|------------------------------------------------------|------------------------------------------------------|------------------------------------------------------------------|------------------------------------------------------------------|----------------------------------------------------|------------------------------------------------------|--------------------------------|
| | Minimum | Maximum | Minimum | Maximum | Minimum | Maximum | |
| Material X | $0,375 \cdot (\% \text{ minimum total deformation})$ | $0,375 \cdot (\% \text{ maximum total deformation})$ | $0,5 \cdot (\% \text{ minimum deformation in radial direction})$ | $0,5 \cdot (\% \text{ maximum deformation in radial direction})$ | $0,5 \cdot (\% \text{ minimum equivalent stress})$ | $0,125 \cdot (\% \text{ maximum equivalent stress})$ | $0,5 \cdot (\% \text{ price})$ |

We can see in Table 5.3 the normalized values for each material.

Table 5.3: Normalized values for each material

| Material | Normalized values | Position |
|-----------------------------------------|-------------------|----------|
| PA66 (50% long glass fiber, lubricated) | 0,714 | 2 |
| PA66 (40% long glass fiber, lubricated) | 0,988 | 6 |
| PA6 (50% long glass fiber) | 0,696 | 1 |
| PA66 (50% glass fiber) | 0,768 | 3 |
| PA66 (40% glass fiber, lubricated) | 1,068 | 7 |
| PA66 (50% long glass fiber) | 0,789 | 4 |
| PA66 (40% long glass fiber) | 1,141 | 8 |
| PA66 (30% glass fiber, lubricated) | 0,961 | 5 |

As we can see, and as previously mentioned, the three most suitable materials to manufacture our impeller were, respectively, PA6 (50% long glass fiber), PA66 (50% long glass fiber, lubricated) and PA66 (50% glass fiber).

For our application, it became very difficult to use a long fiber since the impeller was of small dimensions, therefore, the remaining materials that were left were the following ones.

Table 5.4: New normalized values

| Material | Normalized values | Position |
|------------------------------------|-------------------|----------|
| PA66 (50% glass fiber) | 0,768 | 1 |
| PA66 (40% glass fiber, lubricated) | 1,068 | 3 |
| PA66 (30% glass fiber, lubricated) | 0,961 | 2 |

Since the material choice and the welding method between the parts were related, as shown in Figure 2.3, we chose both at the same time. Therefore, once we talk about the joining technology in the next section, we will choose the manufacturing material of the impeller and the welding method.

5.2. Joining method between parts of the impeller

From section 2.3, we knew that the most chosen option for welding two thermoplastics was ultrasonic welding because thanks to its technology it achieves very precise joints, while achieving a high repeatability in the joints in automated processes. This had an inconvenient, and was that if the application had rounded or circular pieces, it was no longer cheap.

In addition to ultrasonic welding, we also considered vibration welding or heat welding. The second spent more energy when the process was carried out, especially in large pieces, although to use the first one we needed a much more expensive equipment. If we wanted some joints with greater hardness we should use heat welding because of the comments previously mentioned.

If our application required great precision and good surface finish, we should use laser welding, but it was much more expensive than the previous ones and the process time is slower.

Since our material was a polyamide, we checked if it was possible to weld two pieces of the same material in any of the mentioned technologies, and the answer was affirmative. Knowing that the company had already tested heat welding, and that ultrasonic or vibration welding was more expensive, we decided to choose heat welding.

By [8], we knew that the percentage of surrounding material strength was 90%, higher than ABS or polystyrene, although lower than polyethylene or polypropylene. The polyamides had to be completely dry at the time of welding or the formation of froth could be caused. The fillers caused the reduction of the joining force, so that pieces with a percentage of more than 40% filler could not be welded with this method [8].

PA66 (50% glass fiber) was left out of choice despite being the best valued and was then in first place the PA66 (30% glass fiber, lubricated) and secondly the PA66 (40% glass fiber,

lubricated). It is important to bear in mind that the name lubricated means that internal lubricants were added, which improved the already good properties of resistance to wear and friction of the polyamide.

Finally, having evaluated all the records, **the chosen material was the PA66 (30% glass fiber, lubricated)** and the **joining technology between the two pieces** of the impeller was **heat welding**. We can see the overall view in Figure 5.1.

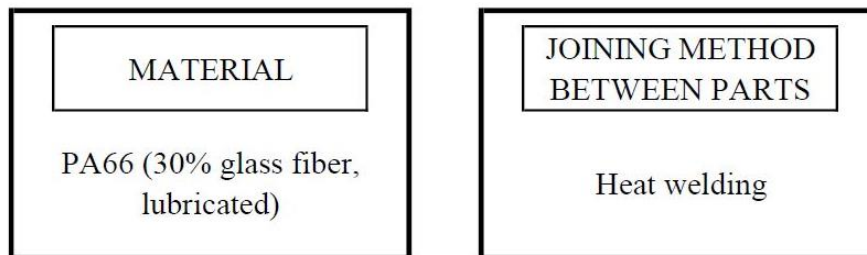


Figure 5.1: Overall view of section 5.1 and 5.2

5.3. Engineering design

In this section we will only discuss the measures for external design, since the internal design was related to the next section.

In order to choose the best external design, the values of Table 4.4 and Table 4.5 were normalized, as was done in section 5.1, applying the same coefficients and changing the price table by the starting torque.

Doing this, the values of the following table were obtained.

Table 5.5: Normalized values for each external design

| Assembly | Normalized values | Position |
|----------|-------------------|----------|
| A1 | 0,264 | 9 |
| A2 | 0,196 | 3 |
| A3 | 0,232 | 5 |
| A4 | 0,233 | 6 |
| A5 | 0,184 | 2 |
| A6 | 0,227 | 4 |
| A7 | 0,783 | 10 |
| A8 | 0,239 | 8 |
| A9 | 0,180 | 1 |
| A10 | 0,238 | 7 |

According to the normalized values of Table 5.5, the three best assemblies were, respectively, A9, A5 and A2.

Finally, **the chosen external design was A9**, and these were its properties for the selected previous material. We can see the overall view in Figure 5.2.

Table 5.6: External design properties (Figure 3.7)

| Assembly | (1) Upper hub diameter [mm] | (2) Cover thickness [mm] | (3) Lower disc thickness [mm] | (5) Lower hub diameter [mm] | (6) Cover hole diameter [mm] | Volume [mm ³] |
|----------|-----------------------------|--------------------------|-------------------------------|-----------------------------|------------------------------|---------------------------|
| A9 | 9,8 | 1,2 | 1,5 | 10,3 | 23,9 | 12330 |

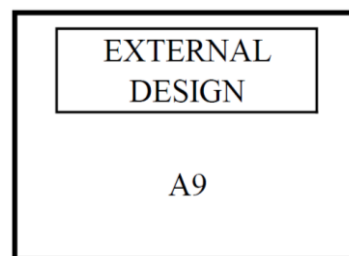


Figure 5.2: Overall view of section 5.3

5.4. Joining method between shaft and impeller

Before discussing the method of joining between the impeller and the shaft, we would like to comment on the results seen in Table 4.6. And as we can see, the vibrations were higher in the case of AS1 than in the others, where the hole was no longer through.

$$\omega = \sqrt{\frac{k}{m}} \quad (5.1)$$

By the equation (5.1), we know that the angular frequency depends on the spring rate and the mass. Therefore, if we varied the mass in our system, the way it vibrated varied. That is, if we increased the mass as is the case of AS1, we increased the vibrations.

So, what we did was calculate a ratio with the values of Table 4.6, in which we took the average between the values of mode 2 and mode 3 of each assembly and the result we subtracted by 1000, which was the frequency with which we worked. We can see the results in Table 5.7.

Table 5.7: Ratio for each internal design

| Assembly | Ratio | Position |
|----------|--------|----------|
| AS1 | 150,37 | 10 |
| AS2 | 141,88 | 9 |
| AS3 | 140,35 | 6 |
| AS4 | 141,50 | 8 |
| AS5 | 137,11 | 2 |
| AS6 | 136,94 | 1 |
| AS7 | 139,94 | 5 |
| AS8 | 139,05 | 4 |
| AS9 | 141,39 | 7 |
| AS10 | 138,35 | 3 |

Therefore, regardless of the joining method chosen between the impeller and the assembly, **the hole was not through and had the depth proposed in AS6, whose hole was made in IBS6 as seen in Table 3.8: Moments of inertia of the assemblies .**

Table 5.8: Internal design properties (Figure 3.7)

| Part | (4) Hole depth [mm] |
|------|---------------------|
| IBS6 | 7,6 |

Now we are going to talk about the choice of joining technology between the shaft and the impeller. As already discussed in section 2.5, this union required a limitation of movement in the axial and radial direction, and that provided a good starting torque.

To do this, we will compare in a table the advantages and disadvantages of each.

Table 5.9: Morphological matrix of joining methods

| Technology | Advantages | Disadvantages |
|-----------------------|---------------------------------------------------|-------------------------------------|
| Adhesive bonding [18] | Decrease in noise and vibrations | Disassembly |
| | Good thermal capabilities | Long-term resistance |
| | Sealing function and protection against corrosion | Preparation and application time |
| | The part does not deform | Security and environment |
| | Well bonding | Surface pre-treatment |
| Laser | Easy automation and greater versatility | Price |
| | Lower risks of contamination of the joint | Risk of damage to components |
| | Speed of joining | Shape limitations |
| | Weight reduction (no additional material) | Surface pre-treatment |
| Inserts | Low technology required | Concentrate loads in certain points |
| | Market availability | Loosening in plastic parts |

| | | |
|----------------|-------------------------------------|-----------------------|
| | Moulding around it | Moisture |
| | Replacement is possible | Reclosure limitations |
| | The part does not deform | Visualize notches |
| New hub design | Cheap | Difficult design |
| | Durable and strong connection | - |
| | Replacement is possible | - |
| | Secondary operations are not needed | - |

Once we have visually the advantages and disadvantages as in the Table 5.9, now it is necessary to apply a weight to different criteria and normalize the results to choose the best method of union.

Table 5.10: Criteria matrix of joining methods

| Criterion | Weight | Adhesive bonding | Laser | Inserts | New hub design |
|--------------------------|--------|------------------|-------|---------|----------------|
| Automation | 3 | 1 | 3 | 3 | 4 |
| Cost | 5 | 2 | 3 | 4 | 4 |
| Dissassembly | 2 | 1 | 1 | 4 | 4 |
| Durability | 4 | 3 | 4 | 3 | 4 |
| Parts deformation | 3 | 5 | 3 | 4 | 4 |
| Secondary operations | 4 | 3 | 2 | 4 | 4 |
| Security and environment | 2 | 1 | 3 | 5 | 4 |
| Thermal capabilities | 3 | 3 | 4 | 3 | 4 |
| Weight reduction | 4 | 2 | 4 | 3 | 4 |
| Sum | | 73 | 93 | 108 | 120 |

Next, we are going to explain how to understand the Table 5.10. Each criterion was assigned a weight from 1 to 5, from least to most importance respectively.

In the other columns we have the four possible joining technologies to choose from, and for each criterion, we have also applied a number from 1 to 5 according to the following criteria. For the degree of automation, a larger number assumed that it was not a manual operation and that it can be manufactured in series. For the costs, a lower value meant that it was more expensive. For the dissassembly, a larger number meant that it was possible to replace it more easily without damage associated with other parts. For the durability of the union, the greater the value, the greater the durability. For the associated deformation of pieces, the higher the value, the less associated damage. For secondary operations, the higher the value, the fewer secondary operations required the union. For safety and taking into account the environment, the higher the value means that there are no operations that may have polluting residues. For thermal capabilities, the higher the value, the better it could withstand high temperatures. Finally, the greater value in weight reduction meant that there were no secondary elements that increased the weight of the system.

In the last row we can see how each product of the weight has been added by the value of each criterion in each technology. Therefore, as we can see in Table 5.10 with the maximum

value, **the new hub design**, commented in section 2.5.4, **will be the selected joining technology between the impeller and the shaft**. We can see the overall view in Figure 5.3.

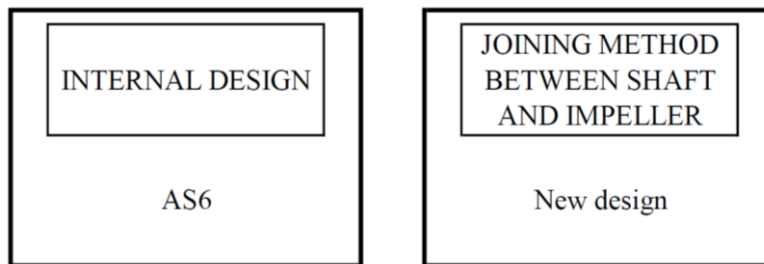


Figure 5.3: Overall view of section 5.4

6. Conclusions

Once exposed the discussions in previous section, some conclusions can be drawn.

- 1) The general objectives and the main objective have been fulfilled, which focused on the study of materials, of new designs through software in 3D modelling, and of selecting a joining technology between the two parts that formed the impeller and another joining between the shaft and the impeller.
- 2) An approximate model of the impeller was used for numerical simulations. Analysis has shown how changing design parameters could affect the deformation and stress level in the impeller. In the best case the maximum stress was reduced by 14,8%.
- 3) Regarding the specific objectives, multiple configurations of the internal design of the hub were generated, in order to achieve the optimal solution seen in section 5.4. Only the most promising option is presented and analysed.
- 4) The most economical and most suitable method for joining the two pieces of the same polymeric material was heat welding. It should be noted that a material was obtained that was not proposed from the beginning and that met very in favour of the specifications that were demanded. As data it should be noted that weight of the new impeller design from PA66 (30% glass fiber, lubricated) was 46% lighter than aluminium, metallic material that is used currently to manufacture the impeller.
- 5) This project can be applied to other techniques in which a metallic material is used and can be replaced by a plastic one. The cost is a very important factor and is that the price in material for making an order of 1000 impellers, does not exceed 80 € (3,88 €/kg).

Before launching the product to be manufactured, and according to the results, we should carry out a new iteration based on numerical calculations and a series of experiments with prototypes to validate calculations and durability.

7. Bibliography

- [1] I. Markič and F. Gačnik, “Impeller from thermoplastic material for vacuum cleaner motors,”. DOMEL HOLDING d.d. Internal report, 2018.
- [2] “HowStuffWorks,” [Online]. Available: <https://home.howstuffworks.com/how-to-repair-small-appliances8.htm>. [Accessed 5th March 2018].
- [3] “Engineering360,” [Online]. Available: https://www.globalspec.com/learnmore/flow_control_flow_transfer/pumps/impellers. [Accessed 5th March 2018].
- [4] K. T. Ulrich and S. D. Eppinger, Product design and development, McGraw-Hill Companies, Inc., 2000.
- [5] V. Mallick, “Thermoplastic composite based processing technologies for high performance turbomachinery components”. Composites Part A: Applied Science and Manufacturing, Vol. 32, Issue 8, Switzerland 5 August 2001, Pages 1167-1173.
- [6] *Granta Design*. CES Edupack (version 2017) [software]
- [7] A. Yousefpour, M. Hojjati and J.-P. Immarigeon, “Fusion Bonding/Welding of Thermoplastic Composites,”. Journal of Thermoplastic Composite Materials, Vol 17, Issue 4, 2004, Pages 303-341.
- [8] J. Rotheiser, Joining of Plastics, Carl Hanser Verlag GmbH & Co. KG, 2009.
- [9] “Forward Technology,” [Online]. Available: <http://www.forwardtech.com>. [Accessed 9th April 2018].
- [10] V. K. Stokes, “Vibration welding of thermoplastics. Part I: Phenomenology of the welding process,”. Polymer Engineering & Science, Vol. 28, Issue 11, June 1988, Pages 718-727.
- [11] “LDM,” [Online]. Available: <https://ldm.la/producto/soldadura-de-plasticos-por-laser/>. [Accessed 12th April 2018].
- [12] B. D. Garrison, “Single piece impeller having radial output”. United States Patent 6,537,030, 25 March 2003.

- [13] R. L. Belonger and D. L. Seuser, “Impeller construction for a centrifugal pump,”. United States Patent, 3,408,944; 1966.
- [14] R. F. Beehler, “Hub for a plastic blower impeller”. United States 24 July 1990.
- [15] *Dassault Systèmes SE*, SolidWorks (version 2017) [software]. (November 1, 1995).
- [16] *Ansys*, Ansys Workbench (version 19.0) [software].
- [17] DuPont, [Online]. Available: <https://dupont.materialdatacenter.com/profiler/main/standard/main/table>. [Accessed 7th May 2018].
- [18] G. K. A. Kodokian and A. J. Kinloch, “Surface pretreatment and adhesion of thermoplastic fibre-composites,”. *Journal of Materials Science Letters*, June 1987, Volume 7, Issue 6, Pages 625-627.